Journal of Medicinal Chemistry

Article

Synthesis and Pharmacology of Willardiine Derivatives Acting as Antagonists of Kainate Receptors

Nigel P. Dolman, Helen M. Troop, Julia C. A. More, Andrew Alt, Jody L. Knauss, Robert Nistico, Samantha Jack, Richard M. Morley, Zuner A. Bortolotto, Peter J. Roberts, David Bleakman, Graham L. Collingridge, and David E. Jane

J. Med. Chem., **2005**, 48 (24), 7867-7881• DOI: 10.1021/jm050584l • Publication Date (Web): 05 November 2005

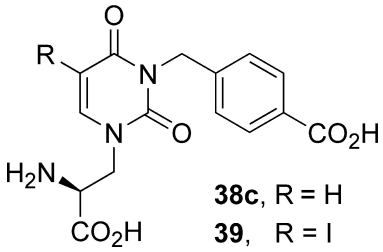

38c, R = H
39, R = I

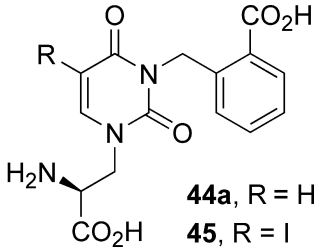

44a, R = H
45, R = I

More About This Article

Additional resources and features associated with this article are available within the HTML version:

- Supporting Information
- Links to the 4 articles that cite this article, as of the time of this article download
- Access to high resolution figures
- Links to articles and content related to this article
- Copyright permission to reproduce figures and/or text from this article

View the Full Text HTML

Journal of Medicinal Chemistry is published by the American Chemical Society. 1155 Sixteenth Street N.W., Washington, DC 20036

Synthesis and Pharmacology of Willardiine Derivatives Acting as Antagonists of Kainate Receptors

Nigel P. Dolman,[†] Helen M. Troop,[†] Julia C. A. More,[†] Andrew Alt,[‡] Jody L. Knauss,[‡] Robert Nistico,[§] Samantha Jack,[†] Richard M. Morley,[†] Zuner A. Bortolotto,[§] Peter J. Roberts,[†] David Bleakman,[‡] Graham L. Collingridge,[§] and David E. Jane*[,†]

Department of Pharmacology, MRC Centre for Synaptic Plasticity, School of Medical Sciences, University Walk, University of Bristol, Bristol, BS8 1TD, U.K., Department of Anatomy, MRC Centre for Synaptic Plasticity, School of Medical Sciences, University of Bristol, BS8 1TD, U.K., and Neuroscience Research, Eli Lilly and Company, Lilly Corporate Center, Indianapolis, Indiana 46285

Received June 20, 2005

The natural product willardiine (**8**) is an AMPA receptor agonist while 5-iodowillardiine (**10**) is a selective kainate receptor agonist. In an attempt to produce antagonists of kainate and AMPA receptors analogues of willardiine with substituents at the N^3 position of the uracil ring were synthesized. The N^3-4-carboxybenzyl substituted analogue (**38c**) was found to be equipotent at AMPA and GLU_{K5}-containing kainate receptors in the neonatal rat spinal cord. The N^3-2-carboxybenzyl substituted analogue (**38a**) proved to be a potent and selective GLU_{K5} subunit containing kainate receptor antagonist when tested on native rat and human recombinant AMPA and kainate receptor subtypes. The GLU_{K5} kainate receptor antagonist activity was found to reside in the *S* enantiomer (**44a**) whereas the *R* enantiomer (**44b**) was almost inactive. 5-Iodo substitution of the uracil ring of **44a** gave **45**, which was found to have enhanced potency and selectivity for GLU_{K5}.

Introduction

It is now widely accepted that (*S*)-glutamate (**1**) is the principal excitatory neurotransmitter in the vertebrate central nervous system (CNS). (*S*)-Glutamate can activate a range of glutamate receptor subtypes, and these have been divided into two general classes: ionotropic glutamate (iGlu) receptors and metabotropic glutamate (mGlu) receptors. The iGlu receptors are ligand gated ion channels, which mediate fast synaptic responses in the CNS. The iGlu receptors include the *N*-methyl-D-aspartate (NMDA), (*S*)-2-amino-3-hydroxy-5-methyl-4-isoxazole-propionic acid (AMPA, **2**), and (2*S*,3*S*,4*S*)-3-carboxymethyl-4-isopropenylpyrrolidine-2-carboxylic acid (kainate, **3**) receptor subtypes.[1,2] While progress has been made in obtaining subtype-selective agonists and antagonists for the various glutamate receptor subtypes, there are very few compounds capable of discriminating between responses mediated by AMPA and kainate receptors.[2] This problem has been exacerbated by the discovery that AMPA receptors are tetramers composed of subunits termed GLU_{A1-4}, which can be combined into functional homo- or heteromeric receptors (IUPHAR nomenclature of the receptors that are also known as GluR1-4 or GluRA-D).[3] Kainate receptors, on the other hand, are composed of GLU_{K5-7}, GLU_{K1}, and GLU_{K2} subunits (IUPHAR nomenclature of the receptors that are also known as GluR5-7, KA1, and KA2).[3] GLU_{K5-7} either alone or in combination with GLU_{K1} or GLU_{K2} subunits form functional ion channels. However, homomeric GLU_{K1} or GLU_{K2} receptors bind kainate with high affinity but do not form functional ion channels.[3]

Only a few examples of selective kainate receptor antagonists have been reported. A series of compounds based around the decahydroisoquinoline nucleus such as LY293558 (**4**), LY382884 (**5**), and **6** have been reported to be competitive GLU_{K5} receptor antagonists.[4,5] These antagonists have been used to provide evidence for a role for GLU_{K5} in hippocampal synaptic plasticity and in a range of CNS disorders such as epilepsy, chronic pain, ischemia, and migraine.[4,5] More recently the first noncompetitive antagonists, such as NS3763 (**7**) which shows selectivity for GLU_{K5}, have been reported.[6]

We have previously reported that in functional assays analogues of the natural product willardiine (**8**) show a degree of AMPA or kainate receptor subunit selectivity.[7] In binding assays, 5-fluorowillardiine (**9**) shows 10−20-fold higher affinity for GLU_{A1} and GLU_{A2} over GLU_{A3} and GLU_{A4} and 70−120-fold selectivity over GLU_{K5}.[8] In contrast (*S*)-5-iodowillardiine (**10**) has high affinity for GLU_{K5} and shows >600-fold selectivity for this subunit versus the AMPA receptor subunits.[8] Thus, 5-substitution of willardiine is a useful way of obtaining selective AMPA or kainate receptor agonists.

Antagonists of AMPA and/or kainate receptors based on an amino acid structure often have a long spacer between the α-carboxylic acid and the terminal acid group. For example, the selective AMPA receptor antagonist (*S*)-ATPO (**11**) has a phosphonomethyl group attached to the oxygen atom on the isoxazole ring of **2**, which has the effect of increasing the inter-acidic group chain length.[9,22] In addition, the AMPA/kainate selective antagonist **4**[10] and the GLU_{K5} selective antagonist **5**[4]

* To whom correspondence should be addressed. Phone: +44 (0)-117 9546451. Fax: +44 (0)117 9250168. E-mail: david.jane@bristol.ac.uk.

† Department of Pharmacology, MRC Centre for Synaptic Plasticity, School of Medical Sciences, University Walk, University of Bristol.

‡ Eli Lilly and Company.

§ Department of Anatomy, MRC Centre for Synaptic Plasticity, School of Medical Sciences, University of Bristol.

10.1021/jm050584l CCC: $30.25
Published on Web 11/05/2005

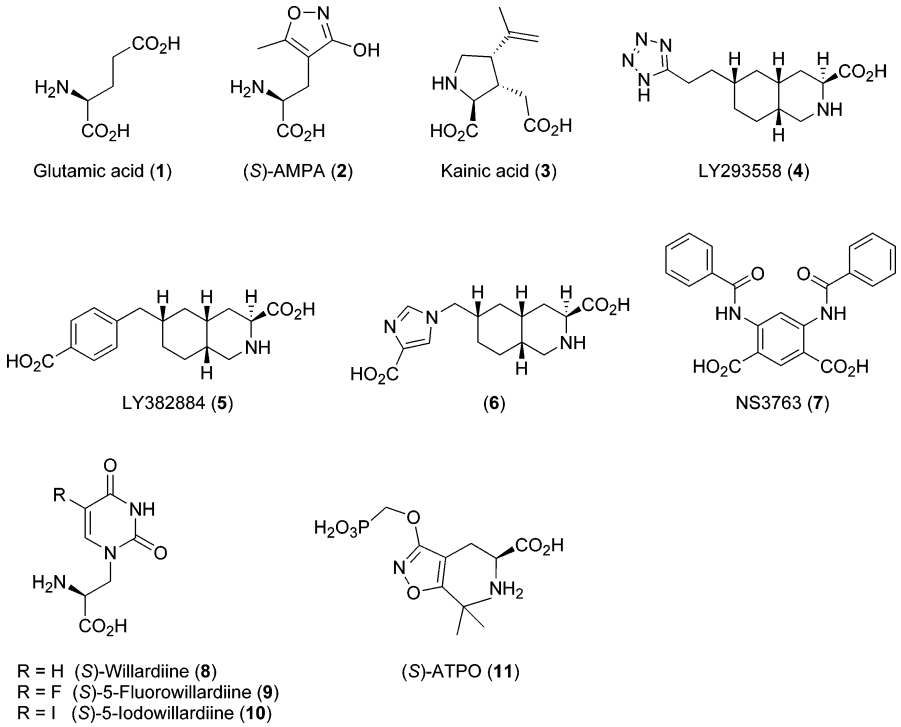

Figure 1. Structures of selected known AMPA and kainate receptor agonists and antagonists.

have a long inter-acidic group chain length compared to the agonists AMPA, kainate, and willardiine.

In an attempt to convert willardiine into a series of selective kainate or AMPA receptor antagonists willardiine analogues were synthesized in which either ionization was blocked by adding a methyl group to the N^3-position of the uracil ring or the inter-acidic group chain length was increased. This series of compounds was then pharmacologically characterized on both cloned and native kainate and AMPA receptors. Pharmacological data for some of these compounds has been published elsewhere.[11]

Results

Chemistry. The N^3-substituted willardiine analogues were conveniently prepared using **12b**[12] as a common starting material. It has been shown previously that the sodium salt **12a** can be alkylated to give predominantly the N^3-substituted product.[13] Initially, we synthesized the 3-methyl analogue (**15**) to ascertain whether prevention of ionization of the uracil ring was sufficient to obtain an antagonist effect. Alkylation of **12a** with iodomethane followed by deprotection in THF/HCl (aq) gave 3-methyluracil (**14**), which had an identical melting point and NMR spectrum when compared to an authentic sample (Scheme 1). Addition of the alanine side chain was carried out via the method previously used for the preparation of willardiine analogues.[8] The sodium salt of **14** was reacted with (*S*)-*N*-Boc-serine-β-lactone[14] (**46**) and the Boc group removed from the intermediate by treatment with TFA to give **15**.

A range of N^3-substituted willardiine analogues were synthesized with methylene spacers of different lengths with a carboxyl group at the end of the chain. Treatment of the sodium salt of **12b** with bromoacetonitrile led to the isolation of the N^3 and N^1 isomers **16** and **17**, respectively, which could be separated by silica gel chromatography. Hydrolysis of **16** and **17** in THF/HCl (aq) gave the corresponding uracils **18** and **21**, the latter having identical properties to an authentic sample. Treatment of the sodium salt of **18** with either (*S*)- or (*R*)-*N*-Boc-serine-β-lactone (**46** or **47**) gave the corresponding (*S*)- or (*R*)-isomers of the N^3-substitued willardiine derivatives **19** and **20**, respectively. Similarly, treatment of the sodium salt of the 1-substituted uracil (**21**) with **46** and subsequent removal of the Boc protecting group with TFA gave the 1-carboxymethyl analogue (**22**). Confirmation of the substitution pattern on the uracil ring of **22** came from nuclear Overhauser effect (NOE) experiments. The CH_2 protons in the N^1-car-

Scheme 1[a]

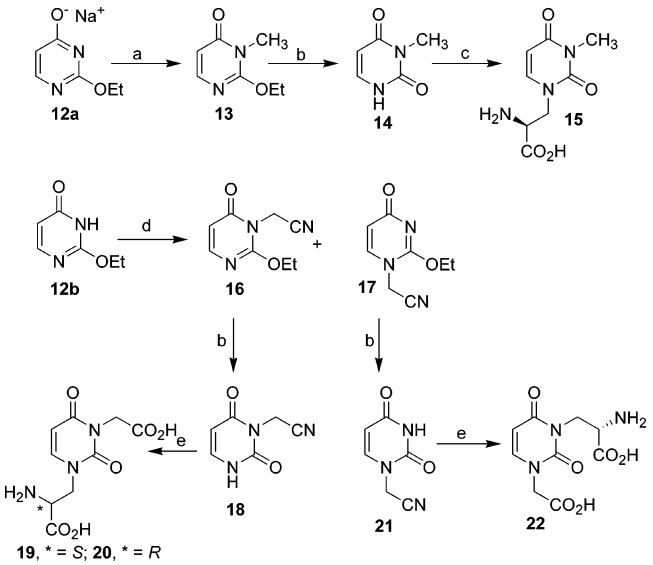

[a] Reagents and conditions: (a) CH_3I, DMF; (b) concentrated HCl/THF (1:9); (c) (i) NaH, DMF, (*S*)-*N*-Boc-serine-β-lactone (**46**), (ii) TFA; (d) NaH, DMF, $BrCH_2CN$, column chromatography; (e) (i) NaH, DMF, (*S*)- or (*R*)-*N*-Boc-serine-β-lactone (**46** or **47**), (ii) 6 M HCl.

Scheme 2[a]

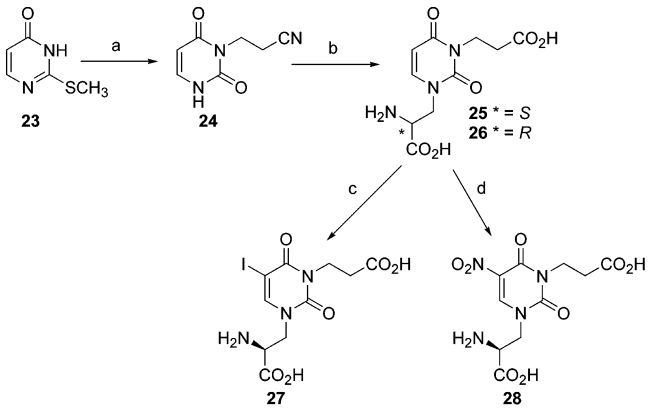

[a] Reagents and conditions: (a) (i) 50% aqueous pyridine, $H_2C{=}CHCN$, (ii) concentrated HCl/H_2O (1:10); (b) (i) NaH, DMF, (*S*)- or (*R*)-*N*-Boc-serine-β-lactone (**46** or **47**), (ii) 6 M HCl; (c) 3 M ICl in 6 M HCl, 70 °C; (d) concentrated H_2SO_4/fuming HNO_3.

Scheme 3[a]

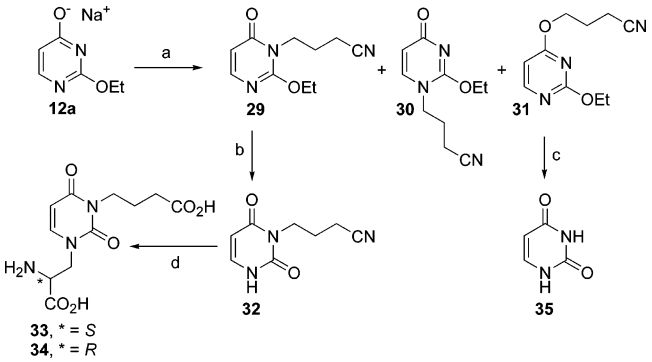

[a] Reagents and conditions: (a) $Br(CH_2)_3CN$, DMF; (b) column chromatography, concentrated HCl/THF (1:9), room temp; (c) column chromatography, concentrated HCl/THF (1:9), reflux; (d) (i) NaH, DMF, (*S*)- or (*R*)-*N*-Boc-serine-β-lactone (**46** or **47**), (ii) 6 M HCl.

boxymethyl analogue (**22**), resonating at 4.7 ppm in the ^{1}H NMR spectrum, were irradiated. As predicted, the signal for the proton at the 6-position of the uracil ring, which is close to the CH_2 group in space, was the only peak in the ^{1}H NMR spectrum to be enhanced.

In order to prepare the *S* and *R* enantiomers of the N^3-2-carboxyethyl derivative, **25** and **26**, respectively, 3-(2-cyanoethyl)uracil (**24**) was synthesized from **23** according to a literature method[15] and the sodium salt of this uracil treated with either **46** or **47** (Scheme 2). The (*S*)-isomer of the 2-carboxethyl analogue (**25**) was iodinated using ICl in 6 M HCl[16] to give the 5-iodo derivative **27** and nitrated using fuming nitric acid to give the 5-nitro derivative **28** (Scheme 2).

Treatment of the sodium salt **12a** with 4-bromobutyronitrile gave the N^3- (**29**), N^1- (**30**), and O^4- (**31**) alkylated products in the ratio of 5:1:4 as deduced by ^{1}H NMR (Scheme 3). Analysis of the N^3- and N^1-alkylated products by ^{1}H NMR revealed that they possessed similar chemical shift patterns to the cyanomethyluracils (**16** and **17**), and thus it was possible to decide which NMR data related to the N^1- and N^3-cyanopropyl uracils. The NMR structural assignment was in agreement with the expected predominance of the N^3-substitued analogue in the product distribution. Although the N^3-alkylated isomer (**29**) could be isolated

Scheme 4[a]

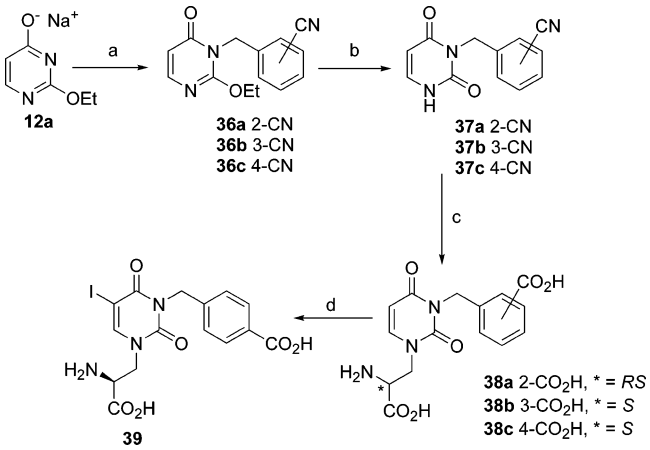

[a] Reagents and conditions: (a) 2-, 3-, or 4-bromomethylbenzonitrile, DMF; (b) column chromatography, concentrated HCl/THF (1:9), room temp; (c) (i) NaH, DMF, (*S*)-*N*-Boc-serine-β-lactone (**46**), (ii) 6 M HCl; (d) 3 M ICl in 6 M HCl, 70 °C.

in the pure form, the N^1-alkylated compound (**30**) could not be purified from contaminating N^3-isomer (**29**). That **31** was the O^4-substituted product was demonstrated by the ease of acid hydrolysis to uracil (**35**). The N^3-substituted derivative **29** was converted to the corresponding uracil (**32**) by acid hydrolysis and the sodium salt of **32** treated with either **46** or **47** to give the corresponding (*S*)- or (*R*)-isomers **33** and **34**, respectively, following acid hydrolysis of the intermediate with 6 M HCl (aq).

Treatment of the sodium salt **12a** with the appropriately substituted bromomethylbenzonitrile gave mainly the N^3-substituted derivative (**36a**−**c**) as deduced from the ^{1}H NMR spectra (Scheme 4). Assignment of the structure of the regioisomers produced in these reactions was based on the chemical shifts for the H^5 and H^6 protons on the uracil ring and the benzylic CH_2, as they were distinctive for the N^1-, N^3-, and O^4-isomers. Compounds **36a**−**c** were hydrolyzed to the intermediate uracils (**37a**−**c**) and the sodium salts of **37a**−**c** treated with (*S*)-*N*-Boc-serine-β-lactone (**46**) to give the required products **38a**−**c** after hydrolysis in 6 M HCl. Iodination of **38c** with 3 M ICl in 6 M HCl gave the corresponding 5-iodo derivative (**39**) in 41% yield (Scheme 4).

In an attempt to corroborate the structural assignment of **38a** and **38b**, NOESY experiments were performed on the N^1-alkylated analogue of **36b** and on **36a**. In the case of the N^1-alkylated analogue of **36b** the benzylic protons show an interaction with the H^6-proton on the uracil ring and lead to an NOE enhancement. In contrast, the benzylic protons of **36a** did not show an interaction with the H^6-proton on the uracil ring as no NOE enhancement was observed.

An NOE experiment was carried out on **38c**, in which the protons belonging to the CH_2 group in the CH_2Ph side chain resonating at 5.15 ppm were irradiated. It was noted that the signal from the proton at the 5-position in the uracil ring that resonates at 6.0 ppm was the only peak to be enhanced. This confirmed that the aromatic side chain is indeed at the N^3-position in the uracil ring and not at the N^1-position.

It was noted that, when **38b** was applied to Dowex AG-1 hydroxide resin, hydrolysis of the uracil ring

Scheme 5[a]

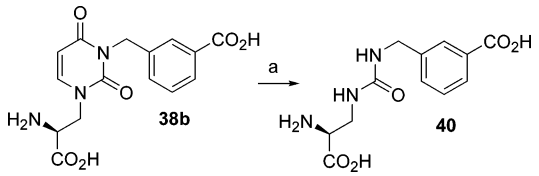

[a] Reagents and conditions: (a) Dowex X18-400 resin (hydroxide form)

Scheme 6[a]

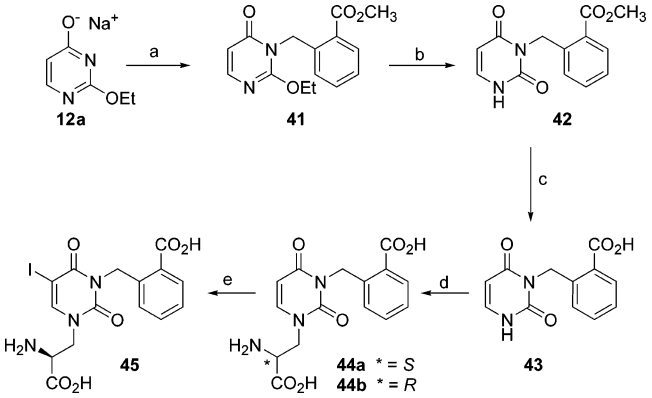

[a] Reagents and conditions: (a) methyl 2-bromomethylbenzoate, DMF; (b) column chromatography, 6 M HCl/acetonitrile; (c) (i) NaOH, EtOH/H_2O, (ii) 1 M HCl; (d) (i) NaH, DMF, (*S*)- or (*R*)-N−Boc-serine-β-lactone (**46** or **47**), (ii) 2 M HCl; (e) ICl in 6 M HCl, 70 °C.

occurred to give the urea **40** (Scheme 5). This is likely due to the strongly basic conditions of the resin column as **40** could also be isolated if **38b** was allowed to stand in aqueous sodium hydroxide. This sensitivity to basic conditions was not observed with any other N^3-substituted willardiine synthesized in this study.

In the case of **38a** the prolonged hydrolysis time required to convert the nitrile to the carboxylic acid led to the isolation of the racemic product. An alternative route was used in order to synthesize the pure *S* enantiomer **44a** (Scheme 6). In this case the sodium salt **12a** was alkylated with methyl 2-bromomethylbenzoate and the N^3-alkylated product (**41**) was separated from the N^1 and O^4-alkyated byproducts by silica gel column chromatography. Hydrolysis of **41** in 6 M aqueous hydrochloric acid in acetonitrile yielded the uracil **42**, which was further hydrolyzed in aqueous sodium hydroxide to give the carboxylic acid (**43**). The di-sodium salt of **43** was treated with **46** to give **44a** after removal of the Boc group in TFA. Analysis by chiral HPLC showed that **44a** had an ee of >99%. The *R* enantiomer **44b** was synthesized in a similar manner. Iodination of **44a** with 3 M ICl in 6 M HCl[16] gave the corresponding 5-iodo derivative (**45**) in 41% yield (Scheme 6).

Pharmacology. In Vitro Electrophysiology. Kainate Receptor Antagonist Activity. To examine antagonist activity at GLU_{K5}-containing kainate receptors, the ability of compounds to depress kainate-induced depolarization of neonatal rat dorsal root C-fibers was assessed (see Table 1 for data).[11] This preparation has been previously shown to express a population of kainate receptors[17] containing the GLU_{K5} subunit.[18] The *S* enantiomers of the N^3-substituted willardiine analogues tested possessed the predominant antagonist activity at kainate receptors. The optimal length for the alkyl chain linker between the N^3-position on the uracil ring and the terminal carboxylic acid group for antagonist activity at kainate receptors was not clear, as a linker of two or three methylene groups, as found in **25** and **33** respectively, led to compounds of similar activity. The use of a benzyl group linker led to compounds **38a**−**c**, with **38a** and **38c** being more potent than the alkyl chain analogues **25** and **33**. A Schild plot was constructed for the ability of compound **38c** to antagonize kainate-induced depolarization of the isolated dorsal root preparation. This gave a pA_2 value of 4.96 and a slope of 1.05 ± 0.05, consistent with a competitive mode of antagonism. The *S* enantiomer **44a** had most of the kainate receptor antagonist activity, with the *R* enantiomer **44b** being almost inactive. Iodination of the 5-position of the uracil ring of compounds **25**, **38c**, and **44a** to give **27**, **39**, and **45**, respectively, improved kainate receptor antagonist activity by approximately the same extent in each case. Compounds **44a** and **45** are potent antagonists of GLU_{K5}-containing kainate receptors expressed on dorsal root C-fibers (K_D values 0.402 ± 0.045 and 0.209 ± 0.019 μM, respectively).

AMPA Receptor Antagonist Activity. The neonatal rat spinal cord preparation was used to assess the potency of the novel N^3-substituted willardiine analogues at native AMPA receptors. The ability of compounds to reduce the fast component of the dorsal root-evoked ventral root potential (fDR-VRP), which is mediated chiefly by AMPA receptors expressed on motoneurons, was used as a fast method of investigating the rank order of antagonist potency at AMPA receptors (see Table 1 for data).[11] The 3-methyl analogue (**15**) did not show antagonist activity but did produce a depolarization when tested at a concentration of 1 mM, suggestive of weak iGluR agonist activity. Thus blocking ionization of the uracil ring of willardiine is not sufficient to convert it into an antagonist as **15** was found to be a weak agonist rather than an antagonist. The agonist activity may be explained by the ability of the 2-oxo group of **15** to interact with the same residues as **8**[23] (Ser654 and Thr655) in the AMPA receptor binding pocket via hydrogen bonds, albeit with lower affinity than **8** itself. The willardiine analogues with an alkyl chain linker between the N^3-position on the uracil ring and the terminal carboxylic acid group were AMPA receptor antagonists with a rank order of potency of **25** > **33** > **19**. The interaction with the AMPA receptor was stereoselective as the *S* enantiomers had the predominant antagonist activity, the corresponding *R* enantiomers **20**, **26**, and **34** having only weak antagonist activity (likely reflecting the small but significant contamination with the *S* enantiomer). Transposing the carboxymethyl and alanine side chains of **19** led to compound **22**, which had weaker antagonist activity at AMPA receptors than the untransposed molecule **19**. As a result of this observation only N^3-substituted willardiine analogues were subsequently synthesized. An improvement in AMPA receptor antagonist potency was obtained when a benzyl group was used as a spacer. The most potent AMPA receptor antagonist in this study was **38c** as it was twice as potent as **25**. A Schild plot was constructed for the ability of **38c** to block depolarization due to **9** (5-fluorowillardiine) on neonatal rat spinal motoneurons.[11] The pA_2 value was 4.48 and

Table 1. Summary of the Activity of Novel N^3-Substituted Willardiine Analogues at AMPA and Kainate Receptors in Electrophysiological and Radioligand Binding Assays[a]

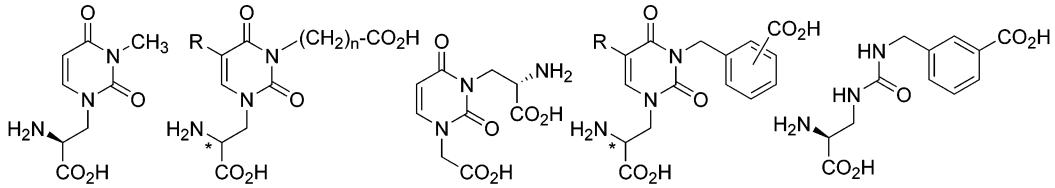

15

19, * = *S*, R = H, n = 1
20, * = *R*, R = H, n = 1
25, * = *S*, R = H, n = 2
26, * = *R*, R = H, n = 2
27, * = *S*, R = I, n = 2
28, * = *S*, R = NO_2, n = 2
33, * = *S*, R = H, n = 3
34, * = *R*, R = H, n = 3

22

38a, 2-CO_2H, * = *RS*, R = H
38b, 3-CO_2H, * = *S*, R = H
38c, 4-CO_2H, * = *S*, R = H
39, 4-CO_2H, * = *S*, R = I
44a, 2-CO_2H, * = *S*, R = H
44b, 2-CO_2H, * = *R*, R = H
45, 2-CO_2H, * = *S*, R = I

40

compound	IC_{50} (μM) vs fDR-VRP[b]	% depression of fDR-VRP at 1 mM[c]	K_D (μM) vs kainate[d]	% reduction of kainate response at 200 μM[e]	K_i (μM) vs [^{3}H]-**9**[f]	K_i (μM) vs [^{3}H]-**48**[g]	GLU_{K6} K_i (μM) vs [^{3}H]kainate[h]
glutamate, **1**							3.28 ± 1.44
AMPA, **2**					0.128 ± 0.001		
kainate, **3**						0.0297 ± 0.0005	0.039 ± 0.007[i]
CNQX, **46**			1.66[j]				1.05 ± 0.07
NBQX, **47**	0.214 ± 0.043		1.78[j]				
15	agonist		nd		nd	nd	>100
19	287 ± 41		nd		195 ± 1	nd	nd
20		44.4 ± 3.0	nd		nd	nd	nd
22		2.9 ± 0.7	nd		>1000	>500	>100
25	23.8 ± 3.9		73.1 ± 4.5		12.9 ± 1.0	>100	>100
26		50.3 ± 1.4		13.2 ± 2.1	166 ± 1	>500	>100
27	13.7 ± 1.7		8.17 ± 1.4		5.0 ± 1.0	52.7 ± 0.6	>100
28	79.9 ± 15.9		nd		nd	nd	>100
33	136 ± 17		60.5 ± 4.1		17.8 ± 1.2	96.2 ± 0.8	>1000
34		61.3 ± 4.9		22.8 ± 9.6	149 ± 1	>500	nd
38a	97.6 ± 9.2		1.09 ± 0.10		nd	nd	>1000
38b		90.2 ± 4.4	49.1 ± 0.5		nd	nd	>1000
38c	10.3 ± 2.4		9.25 ± 0.54		13.4 ± 1.0	>200	>100
39	164 ± 25		5.94 ± 0.63		269 ± 1	>1000	>100
40	>1000		nd		nd	nd	nd
44a	106 ± 13		0.402 ± 0.045		nd	nd	>1000
44b	>100		>100		nd	nd	>1000
45	74.1 ± 4.3		0.209 ± 0.019		nd	nd	>100

[a] All values are from three independent experiments and are expressed as the mean ± SEM; nd = not determined. [b] Depression of the fast component of the dorsal root evoked ventral root potential (fDR-VRP) is a measure of antagonist activity on AMPA receptors expressed on motoneurons. [c] The percentage depression of the fDR-VRP by 1 mM of test antagonist was used for compounds that had only weak AMPA receptor antagonist activity. [d] Apparent K_D values for antagonism of kainate induced depolarization of isolated dorsal root C-fibers calculated using the Gaddum−Schild equation. [e] The percentage depression of a kainate response on isolated dorsal root by 200 μM of test antagonist was used for compounds that had only weak kainate receptor antagonist activity. [f] The K_i value for the inhibition of [^{3}H]-**9** binding refers to a binding experiment for AMPA receptors on rat brain membranes. [g] The K_i value for the inhibition of [^{3}H]SYM2081 ([^{3}H]-**48**) binding refers to a binding experiment for kainate receptors on rat brain membranes. [h] The K_i value for the inhibition of [^{3}H]kainate binding to rat GLU_{K6} expressed on HEK293 cell membranes. [i] K_D value obtained from saturation binding study of [^{3}H]kainate binding to rat GLU_{K6} expressed on HEK293 cell membranes. [j] Values taken from ref 43.

the slope was 1.11 ± 0.13, suggestive of a competitive mode of antagonism. The urea analogue (**40**) of compound **38b** was inactive at AMPA receptors. Iodination of the 5-position of the uracil ring of compounds **25** and **38c** produced differential effects on the AMPA receptor antagonist activity of the resultant compounds. Thus, **27** was almost twice as potent as the parent compound **25**, while **39** was ~16-fold less potent than **38c**. The 5-nitro analogue (**28**) was less potent than the parent compound (**25**) as an AMPA receptor antagonist. The *S* isomer (**44a**) of **38a** and the 5-iodo analogue (**45**) were both weak AMPA receptor antagonists. Compounds **44a** and **45** are therefore selective antagonists of native GLU_{K5}-containing kainate receptors vs AMPA receptors.

Electrophysiology in Hippocampal Slice. Mossy fiber long-term potentiation (LTP) is induced when a high-frequency tetanus is applied to the mossy fiber pathway of the hippocampus, and is manifested as a long lasting enhancement of synaptic strength at the mossy fiber to CA3 synapse.[4c,11c] This form of LTP is not dependent on the activation of NMDA receptors, but is thought to require activation of GLU_{K5}-containing kainate receptors.[4c] We have previously reported that the racemic mixture **38a** blocks NMDA receptor independent mossy fiber LTP at a concentration of 1 μM.[11c] The stereoselectivity of this effect was demonstrated by showing that mossy fiber LTP was blocked by 300 nM **44a**, the *S*-enantiomer, but could be evoked in the presence of 10 μM **44b**, the *R*-enantiomer (Figure 2).

Calcium Fluorescence Assays. Compound **38a** was tested in a functional assay on a range of recombinant kainate and AMPA receptor subunits to confirm the

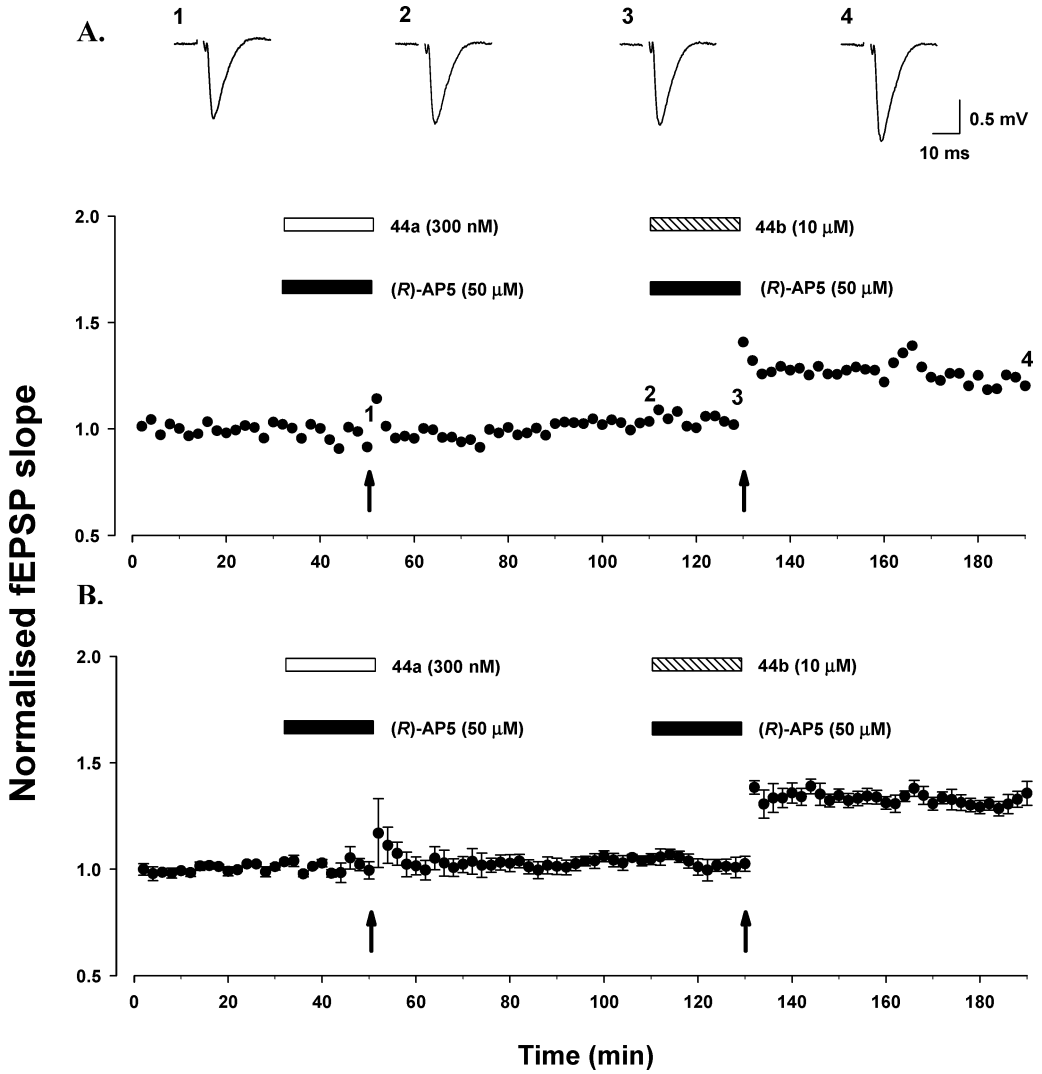

Figure 2. Stereoselective block of mossy fiber LTP. Mossy fiber LTP is blocked in the presence of 300 nM **44a** ($n = 3$) but can be evoked in the presence of **44b** (10 μM) ($n = 5$). (A) A single example to show that mossy fiber LTP is blocked in the presence of 300 nM **44a** but can be evoked in the presence of 10 μM **44b**. Drugs were applied as indicated by the bars and tetani of 100 shocks at 100 Hz were delivered, in the presence of the NMDA receptor antagonist (*R*)-AP5, at the times indicated by arrows. Each point represents the average of 4 successive measurements of the gradient of the field excitatory postsynaptic potential (fEPSP slope). The data were normalized with respect to the 30 min baseline preceding drug application. The traces above the graph show fEPSPs recorded at the time points indicated by the corresponding numbers in the graph. (B) Pooled data for all equivalent experiments. It is clear that a long-term increase in the magnitude of the fEPSP slope (indicative of LTP) is observed after a tetanus is applied in the presence of 10 μM **44b** and (*R*)-AP5, but not in the presence of 300 nM **44a**. This suggests that mossy fiber LTP requires activation of GLU_{K5}-containing kainate receptors but not NMDA receptors.

selective kainate receptor antagonist activity identified in the electrophysiological assays described above.

Recombinant Human AMPA and Kainate Receptor Subtypes. Compound **38a**, when tested on HEK293 cells expressing homomeric human GLU_{K5}, GLU_{K5}/GLU_{K2}, and GLU_{K5}/GLU_{K6}, was shown to have K_b values of 0.6 ± 0.1, 1.0 ± 0.4 and 0.8 ± 0.1 μM, respectively, for blocking glutamate-induced calcium influx. However, **38a** had no effect on calcium influx in cells expressing GLU_{K6} or GLU_{K6}/GLU_{K2} up to a concentration of 300 μM. Compound **38a** had no effect up to a concentration of 300 μM at homomeric human GLU_{A1}, GLU_{A2}, GLU_{A3}, or GLU_{A4} expressed in HEK293 cells in the glutamate-induced calcium influx assay. Thus compound **38a** is a potent antagonist of GLU_{K5} containing kainate receptors showing >300-fold selectivity for these receptors over GLU_{K6} kainate receptor subunits and GLU_{A1-4} AMPA receptor subunits.

Binding Studies. Recombinant Homomeric Rat GLU_{K6} and Human GLU_{K7} Receptors. A number of the novel N^3-substituted willardiine analogues were tested in [^{3}H]kainate displacement binding assays on rat GLU_{K6Q}-transfected HEK293 membranes (see Table 1). A K_D value of 39.0 ± 6.9 nM ($n = 3$) for kainate and a B_{max} value of 1.53 ± 0.43 pmol mg^{-1} protein was determined from a saturation binding analysis of kainate binding to GLU_{K6}. Two standard compounds, glutamate and 6-cyano-7-nitroquinoxaline-2,3-dione (CNQX, **46**), inhibited [^{3}H]kainate binding with K_i values that are similar to published data.[21]

None of the N^3-substituted willardiine analogues tested (see Table 1) showed significant affinity for GLU_{K6}, displaying K_i values of >100 μM in [^{3}H]kainate displacement binding assays on GLU_{K6}. Thus, since compounds **38a**, **39**, **44a**, and **45** were relatively potent

GLU_{K5} receptor antagonists, they show useful selectivity for rat GLU_{K5} over GLU_{K6} receptors.

Compound **38a** inhibited [^{3}H]kainate binding from HEK293 cell membranes expressing human GLU_{K7} receptors with an IC_{50} value of 880 ± 268 μM. Using the Cheng−Prusoff equation a K_i value of 374 ± 122 μM was calculated. In a similar assay 2,3-dihydroxy-6-nitro-7-sulfamoyl-benzo[*f*]quinoxaline (NBQX, **47**), which was used as a positive control, inhibited [^{3}H]kainate binding with an IC_{50} value of 44 ± 20 μM and a K_i value of 18 ± 8 μM, which was similar to the previously reported K_i value of 24 μM.[39] Thus compound **38a** shows >350-fold selectivity for human GLU_{K5} vs GLU_{K7}.

Native AMPA and Kainate Receptors. A number of the novel N^3-substituted willardiine analogues were tested in displacement binding assays on native AMPA or kainate receptors expressed in rat forebrain (see Table 1). In a displacement binding assay using [^{3}H]-(*S*)-5-fluorowillardiine ([^{3}H]-**9**) the K_i value obtained for AMPA (**2**) was consistent with a previous report.[19] In a displacement binding assay on native kainate receptors using [^{3}H](2*S*,4*R*)-4-methylglutamate ([^{3}H]SYM2081, [^{3}H]-**48**), kainate yielded a K_i value that is similar to a previously reported value.[20] In general, K_i values for the binding of the N^3-substituted willardiine analogues to AMPA receptors followed the same rank order of potency as that observed in functional studies (i.e. the fDR-VRP assay) on AMPA receptors expressed on neonatal rat motoneurons. However, K_i values for displacement of [^{3}H]-**48** did not correlate with activity of compounds on GLU_{K5} containing kainate receptors expressed in the dorsal root. Only compound **27** showed significant inhibition of [^{3}H]-**48**, most compounds having K_i values >100 μM, including compound **39**, which was one of the most potent antagonists tested at GLU_{K5} containing kainate receptors in the dorsal root. It has been reported that **48** shows excellent selectivity for GLU_{K5}/GLU_{K6} versus AMPA receptors.[26] Thus, in this binding assay the ability of compounds to inhibit binding to either GLU_{K5} or GLU_{K6} would be expected to be evaluated. As **39**, one of the most potent GLU_{K5} receptor antagonists, failed to inhibit [^{3}H]-**48** binding, it is likely that GLU_{K5} receptors have a low expression level in adult rat forebrain. In support of this conclusion we have also observed that the potent GLU_{K5} agonists **10** and (*S*)-5-trifluoromethylwillardiine fail to inhibit [^{3}H]-**48** binding to rat forebrain.[27] A study of the binding of [^{3}H]ATPA, a GLU_{K5} selective agonist, also concluded that binding affinity to rat brain forebrain was weak.[28] Compound **27** inhibited [^{3}H]-**48** binding with a K_i value of 52.7 μM. The subunit composition of the kainate receptor that **27** is binding to in rat forebrain is not known. It is not likely to be homomeric GLU_{K6} as **27** had a K_i value of >100 μM for inhibition of [^{3}H]kainate from GLU_{K6}. The most likely explanation is that a heteromeric kainate receptor is present in forebrain, as it has been shown that heteromeric kainate receptors can display different pharmacology to receptors containing only one type of kainate receptor subunit.[29]

Discussion

Our previous structure−activity studies on willardiine have concentrated on the effect of adding substituents to the 5-position of the uracil ring on agonist activity at AMPA and kainate receptors.[7,8] In this study a range of N^3-substituted willardiine analogues were synthesized with the aim of determining the structural requirements necessary to convert willardiine into an antagonist at either kainate or AMPA receptors. Although **25**, **27**, and **38c** showed moderate potency as AMPA receptor antagonists, the most significant finding of this study was that some compounds displayed potent and selective antagonist activity on GLU_{K5}-containing kainate receptors.

The isolated dorsal root was used to test compounds for kainate receptor antagonist activity as C-fibers within the root express GLU_{K5}-containing kainate receptors but not AMPA or GLU_{K6}-containing kainate receptors.[11] The presence of GLU_{K5} subunits in kainate receptors expressed on DRG cells has been confirmed by the observation that the previously reported AMPA receptor antagonist **4**[24] is an antagonist at homomeric GLU_{K5} but not GLU_{K6} and also antagonizes the effects of kainate on DRG neurons.[25] We found that only *S* enantiomers of N^3-substituted willardiine analogues had antagonist activity at kainate receptors in this preparation (any activity of the *R* enantiomer likely reflects the small but significant contamination with the *S* enantiomer). The preferred chain length of the linker attached to the N^3-position for optimal antagonism of native GLU_{K5} receptors was not clear as a linker of either 2 or 3 methylene groups was almost equally accommodated by the receptor. Incorporation of a benzyl spacer led to increases in potency at GLU_{K5} receptors when the terminal carboxylic acid group was at the 2- or 4-position of the benzene ring (**38a** and **38c**, respectively). When tested on native AMPA receptors expressed on neonatal rat motoneurons, it was apparent that **38c** was almost equipotent at AMPA and kainate receptors while **38a**, one of the most potent GLU_{K5}-containing kainate receptor antagonists tested, displayed approximately 90-fold selectivity for kainate vs AMPA receptors (see Table 1). We have previously reported that **38a** (50 μM) displayed no antagonist activity at NMDA and group I (mGlu1 and 5) mGlu receptors expressed on neonatal rat motoneurons.[11] Thus in electrophysiological assays **38a** displays remarkable selectivity for GLU_{K5}-containing kainate receptors having little or no activity at AMPA, NMDA, or group I metabotropic glutamate receptors. Tests on recombinant human AMPA and kainate receptor subunits confirmed that **38a** was a selective GLU_{K5} antagonist and showed that the affinity for GLU_{K5} is not changed when the GLU_{K5} subunit is incorporated into a heteromeric assembly with either GLU_{K6} or GLU_{K2}. The potency of **38a** at human recombinant GLU_{K5} (calcium fluorescence assay) correlates well with the activity of this compound at GLU_{K5}-containing kainate receptors in neonatal rat dorsal root. As **38a** had little or no activity on human GLU_{K6}, GLU_{K6}/GLU_{K2}, GLU_{K7}, or rat GLU_{K6} it can be concluded that it is a highly selective GLU_{K5}-containing kainate receptor antagonist. As **38a** was a racemic mixture, we decided to synthesize the separate enantiomers. The *S* enantiomer **44a** had the predominant antagonist activity at native GLU_{K5} kainate receptors while the *R* enantiomer **44b** was found to be inactive. In addition, **44b** was inactive on native AMPA and rat GLU_{K6} receptors.

An increase in potency was observed when the 5-iodo analogues of **25**, **38c**, and **44a** were tested on kainate receptors on dorsal root. Thus, **45** was the most potent GLU_{K5} receptor antagonist in this study, being twice as potent as **44a**. Compounds **39**, **44a**, and **45** failed to inhibit binding in a [^{3}H]kainate displacement binding assay on rat GLU_{K6} in HEK293 cell membranes, suggesting that they are selective for GLU_{K5} vs GLU_{K6}. In addition, **45** had only weak activity in an assay on native AMPA receptors therefore displaying a ~350-fold selectivity for native GLU_{K5}-containing kainate vs AMPA receptors (see Table 1). For this series of antagonists the switch in selectivity between AMPA and GLU_{K5} receptors is less pronounced upon 5-iodo substitution than that observed for willardiine-based agonists, where for instance 5-iodo substitution of willardiine leads to a massive swing to selectivity for GLU_{K5}.[7d,8] This difference may be due to the significant reshaping of the binding pocket between open and closed conformations of the ligand binding core which is evident from X-ray crystal structures.

The GLU_{K5} receptor antagonists identified in this study (**38a**, **44a**, and **45**) are more potent and selective than the previously described decahydroisoquinoline antagonists **4** and **5**. In addition, **45** is of comparable potency to **6**, which is the most potent GLU_{K5} receptor antagonist so far reported. Solutions of the monosodium salt of **45** are stable for at least a week if stored frozen and have been used without any decomposition in in vitro electrophysiological experiments. We have not yet established whether **45** would be stable if given systemically.

In addition to experiments in the spinal cord, the mossy fiber LTP study also affirmed the stereoselectivity of willardiine-based antagonists. We have previously shown using the racemate **38a** that GLU_{K5}-containing kainate receptors are involved in the induction of mossy fiber LTP.[11c] We have shown in this study that mossy fiber LTP was blocked by 300 nM **44a** but in the same experiment could be evoked in the presence of **44b** (10 μM), thus demonstrating that the *S*-form is the active enantiomer. The ability of **44a** to block mossy fiber LTP at 300 nM demonstrates that it is more potent than **38a** at blocking this effect. This is in accordance with the different potencies of these compounds for antagonizing GLU_{K5}-containing receptors, providing further evidence that the GLU_{K5} receptor is involved in the induction of mossy fiber LTP.

Conclusion

A range of novel N^3-substituted willardiine analogues have been shown to be kainate and/or AMPA receptor antagonists. Two compounds, **27** and **38c**, were moderately potent AMPA receptor antagonists, but both these compounds also antagonized GLU_{K5}-containing kainate receptors to a similar extent. More importantly, compounds **38a**, **44a**, and **45** were potent and selective GLU_{K5} receptor antagonists. These three compounds are likely to be useful as pharmacological tools to study the physiological and pathophysiological roles of GLU_{K5}-containing kainate receptors. Indeed compounds **38a** and **44a** have already been used to provide evidence for a role for GLU_{K5}-containing kainate receptors in mossy fiber LTP.

Experimental Section

Chemistry. General Procedures. Proton NMR spectra were measured on a JEOL NMR spectrometer at either 300.40 or 270.18 MHz. Carbon NMR spectra were run on a 300.40 MHz JEOL NMR spectrometer at 75.45 MHz or a 270.18 MHz JEOL spectrometer at 67.94 MHz. 3-(Trimethylsilyl)propionic-2,2,3,3-d_4 acid sodium salt in D_2O and tetramethylsilane in $CDCl_3$, DMSO-d_6, and TFA-*d* were used as internal standards. Elemental analyses were performed in the microanalytical laboratory in the Department of Chemistry, University of Bristol, Bristol, U.K. Melting points were determined in capillary tubes on Electrothermal IA9100 electronic melting point equipment, and are uncorrected. Rotations were carried out in 6 M HCl at room temperature in a cell with a 5 cm path length, with a wavelength of 589 nm at Tocris Cookson Ltd. Thin-layer chromatography was performed on Merck silica gel 60 F_{254} plastic sheets. Silica gel for flash chromatography was silica gel 60 (220−440 mesh) from Fluka chemicals, U.K. The eluents for thin-layer chromatography of amino acids included [2(pyridine:acetic acid:water (3:8:11)):3(*n*-butanol)] and [propan-2-ol:35% aqueous ammonia (70:30)]. Amino acids were detected by spraying plates with a 2% solution of ninhydrin in 70% ethanol. Purity of amino acids was also determined by high voltage paper electrophoresis, using pH 4 buffer and an applied voltage of 4 kV. Ion-exchange resin chromatography was carried out using Dowex 50WX8-400 acid form resin and the acetate or hydroxide form of Dowex X18-400 obtained from Aldrich Chemical Co., U.K., or Biorad AG1X8 from Bio-Rad, U.K. Chiral HPLC analysis was carried out using a Crownpak column, flow rate of 0.5 mL/min, detection 270 nm, 2 °C in pH 1 perchloric acid. For compounds **38a**, **38b**, **39**, **40**, **44a**, and **45** chiral HPLC was carried out using a RSTech, Chirosil RCA+, 150 × 4.6 column, flow rate 1.0 mL/min, detection 220 nM with a mobile phase consisting of methanol/5 mM perchloric acid (85:15). All solids were dried over P_2O_5 in vacuo for 3 days prior to reaction. All anhydrous reactions were conducted under argon. All reagents and dry solvents were obtained from the Aldrich Chemical Co., U.K., unless otherwise stated.

3-Methylpyrimidine-2,4-dione (14). The sodium salt of 2-ethoxypyrimidin-4-one[12] (**12a**) (3.0 g, 20 mmol) was dissolved in dry DMF (60 mL) under a dry nitrogen atmosphere. Iodomethane (2.84 g, 20 mmol) in dry DMF (20 mL) was added portionwise and the mixture left at room temperature for 20 h. Glacial acetic acid (3 mL) was added and the mixture evaporated under reduced pressure to give 2-ethoxy-3-methylpyrimidin-4-one (**13**) as a white solid. The compound was used without further purification in the subsequent reaction. 2-Ethoxy-3-methylpyrimidin-4-one (**13**) was dissolved in concentrated hydrochloric acid/tetrahydrofuran (1:10, 150 mL). After stirring for 20 h at room temperature, the solvent was removed under reduced pressure and the residue was flash chromatographed over silica gel. Elution with ethyl acetate gave **14** (1.65 g, 65%) as a white solid: mp 178.5−179.2 °C; lit. mp 179 °C.[30]

(*S*)-1-(2-Amino-2-carboxyethyl)-3-methylpyrimidine-2,4-dione (15). 3-Methylpyrimidine-2,4-dione (**14**) (1.0 g, 7.93 mmol) was dissolved in dry DMF (30 mL) under a dry nitrogen atmosphere. A 60% suspension of sodium hydride in mineral oil (0.32 g, 7.93 mmol) was added portionwise. After stirring at room temperature for 20 h (*S*)-3-(*t*-butoxycarbonylamino)-oxetan-2-one (**46**) (1.48 g, 7.93 mmol) was added. The mixture was stirred for 20 h, and then the solvent was removed under reduced pressure and the residue suspended in TFA (50 mL). After stirring for 20 h at room temperature with the exclusion of atmospheric moisture the mixture was evaporated under reduced pressure and the residue applied to a column of Dowex 50WX8-400 (0.25 mmol of cation/mL resin; 32 mL). The column was eluted with water and then 1 M aqueous pyridine. The ninhydrin positive fractions of the 1 M aqueous pyridine eluate were combined and evaporated to dryness under reduced pressure. The residue was dissolved in the minimum amount of water and applied to a column of Dowex X18-400 acetate form resin (70 mL). The column was eluted with water and

then aqueous acetic acid of concentrations 0.01, 0.05, 0.1, and 0.3 M. The ninhydrin positive fractions of the 0.3 M aqueous acetic acid eluate were combined and evaporated under reduced pressure. Crystallization of the residue from water gave **15** (0.48 g, 28%) as a yellow solid: mp 179.9−180.9 °C (dec); $[\alpha]_D^{20} = -34.0$ (*c* 0.5, 6 M HCl); ee 98% as determined by chiral HPLC.

3-Cyanomethyl-2-ethoxypyrimidin-4-one (16) and 1-Cyanomethyl-2-ethoxypyrimidin-4-one (17). 2-Ethoxypyrimidin-4-one (**12b**) (4.93 g, 35.2 mmol) was dissolved in dry DMF (100 mL) under a dry nitrogen atmosphere. A 60% suspension of sodium hydride in mineral oil (1.41 g, 35.2 mmol) was added to the stirred solution portionwise. After stirring the mixture for 20 h at room temperature, a solution of bromoacetonitrile (2.5 mL, 35.7 mmol) in dry DMF (30 mL) was added dropwise and the mixture heated to 50 °C for 24 h. The solvent was removed under reduced pressure (1 mmHg) and the residue triturated with diethyl ether and petroleum ether. The solid was flash chromatographed over silica gel. Elution with petroleum ether/ethyl acetate (60:40) gave **16** (3.0 g, 48%) and **17** (1.2 g, 20%).

3-Cyanomethylpyrimidine-2,4-dione (18). 3-Cyanomethyl-2-ethoxypyrimidin-4-one (**16**) (2.8 g, 20 mmol) was dissolved in concentrated hydrochloric acid/THF (200 mL, 1:10). After stirring for 20 h at room temperature, the solvent was evaporated under reduced pressure and the residue crystallized from ethyl acetate to give **18** (2.2 g, 92%).

(*S*)-1-(2-Amino-2-carboxyethyl)-3-carboxymethylpyrimidine-2,4-dione (19). 3-Cyanomethylpyrimidine-2,4-dione (**18**) (2.2 g, 10 mmol) was dissolved in dry DMF (60 mL) under a dry nitrogen atmosphere. A 60% suspension of sodium hydride in mineral oil (0.57 g, 10 mmol) was added portionwise. After stirring for 20 h at room temperature (*S*)-3-(*t*-butoxycarbonylamino)oxetan-2-one (**46**) (2.62 g, 10 mmol) was added portionwise. Stirring was continued for 20 h at room temperature, and then glacial acetic acid (3 mL) was added and the mixture evaporated under reduced pressure. 6 M hydrochloric acid (50 mL) was added to the residue and the mixture heated under reflux for 2 h. The solvent was removed under reduced pressure and the residue applied to a column of Dowex 50WX8-400 (0.25 mmol of cation/mL resin; 80 mL). The column was eluted with water and then 1 M aqueous pyridine. The ninhydrin positive fractions of the 1 M aqueous pyridine eluate were combined and evaporated to dryness under reduced pressure. The residue was dissolved in the minimum amount of water and applied to a column of Dowex X18-400 acetate form (100 mL). The column was eluted with water and then aqueous acetic acid of increasing concentrations of 0.01, 0.05, 0.1, 0.5, and 1 M. The ninhydrin positive fractions of the 1 M aqueous acetic acid eluate were combined and evaporated under reduced pressure. Crystallization of the residue from water yielded **19** (1.23 g, 34%) as a white solid: mp 219.0−221.1 °C (dec); $[\alpha]_D^{20} = -10.5$ (*c* 0.4, 6 M HCl); ee 99% as determined by chiral HPLC.

(*R*)-1-(2-Amino-2-carboxyethyl)-3-carboxymethylpyrimidine-2,4-dione (20). Following the procedure by which **19** was synthesized, treating 3-cyanomethylpyrimidine-2,4-dione (**18**) (0.33 g, 2.16 mmol) in dry DMF (20 mL) with a 60% suspension of sodium hydride in mineral oil (0.09 g, 2.16 mmol), then with (*R*)-3-(*t*-butoxycarbonylamino)oxetan-2-one (**47**) (0.41 g, 2.16 mmol), gave **20** (0.047 g, 8%) as a white solid: mp 207.6−210.7 °C (dec); $[\alpha]_D^{20} = +23.4$ (*c* 1.24, 6 M HCl); ee 98% as determined by chiral HPLC.

(*S*)-3-(2-Amino-2-carboxyethyl)-1-carboxymethyl-pyrimidine-2,4-dione (22). 1-Cyanomethyl-2-ethoxypyrimidin-4-one (**17**) (4.24 g, 23 mmol) was dissolved in concentrated hydrochloric acid/THF (100 mL, 1:10). After stirring for 20 h at room temperature, the solvent was evaporated under reduced pressure and the residue crystallized from ethyl acetate to give 1-cyanomethylpyrimidine-2,4-dione (**21**) (2.6 g, 73%): ^{1}H NMR (300.4 MHz, DMSO-d_6) δ 4.86 (s, 2H, CH_2-CN), 5.67 (d, J = 7.9 Hz, 1H, HCC*H*CO), 7.8 (d, J = 7.9 Hz, 1H, *H*CCHCO); ^{13}C NMR (75.45 MHz, DMSO-d_6) δ 35.83, 102.17, 115.85, 144.48, 150.42, 163.47. ^{1}H NMR data similar to that previously reported for compound **21**.[31]

Following the procedure by which **19** was synthesized, treating 1-cyanomethylpyrimidine-2,4-dione (**21**) (2.4 g, 16 mmol) in dry DMF (60 mL) with a 60% suspension of sodium hydride in mineral oil (0.64 g, 16 mmol) and then with (*S*)-3-(*t*-butoxycarbonylamino)oxetan-2-one (**46**) (3.0 g, 16 mmol) gave **22** (0.28 g, 5%) as a white solid: mp 226.0−227.9 °C (dec); $[\alpha]_D^{20} = -16.93$ (*c* 0.48, 6 M HCl); ee 86% as determined by chiral HPLC.

3-(2-Cyanoethyl)pyrimidine-2,4-dione (24). 2-Methylthiopyrimidin-4-one[32] (**23**) (6.0 g, 0.042 mol) was dissolved in 50% aqueous pyridine (180 mL). Acrylonitrile (30 mL, 0.46 mol) was added and the mixture heated under reflux for 7 h. The solvent was evaporated under reduced pressure to give a white solid, which was rinsed with water and filtered to give 3-(2-cyanoethyl)-2-methylthiopyrimidin-4-one (7.03 g, 86%) as a white solid: mp 102.6−104.8 °C; lit. mp 100−102 °C;[33] ^{1}H NMR (300.4 MHz, DMSO-d_6) δ 2.57 (s, 3H, CH_3), 3.0 (t, J = 6.7 Hz, 2H, CH_2CN), 4.23 (t, J = 6.7 Hz, 2H, N−CH_2), 6.23 (d, J = 6.4 Hz, 1H, HCC*H*CO), 7.87 (d, J = 6.4 Hz, 1H, *H*CCHCO). 3-(2-Cyanoethyl)-2-methylthiopyrimidin-4-one (3.0 g, 0.015 mol) was dissolved in concentrated hydrochloric acid/water (1:10, 12 mL) and heated under reflux for 5 min. The solvent was evaporated under reduced pressure to give **24** (2.22 g, 90%) as white crystals: mp 139.8−143.4 °C; lit. mp 141−142 °C.[34]

(*S*)-1-(2-Amino-2-carboxyethyl)-3-(2-carboxyethyl)pyrimidine-2,4-dione (25). Following the procedure by which **19** was synthesized, treating 3-(2-cyanoethyl)pyrimidine-2,4-dione (**24**) (2.5 g, 15 mmol) in dry DMF (80 mL) with a 60% suspension of sodium hydride in mineral oil (0.61 g, 15 mmol) and then with (*S*)-3-(*t*-butoxycarbonylamino)oxetan-2-one (**46**) (2.83 g, 15 mmol) gave **25** (2.36 g, 58%) as a white solid: mp 212.5−214.4 °C (dec); $[\alpha]_D^{20} = -24$ (*c* 1.0, 6 M HCl); ee 93% as determined by chiral HPLC.

(*R*)-1-(2-Amino-2-carboxyethyl)-3-(2-carboxyethyl)pyrimidine-2,4-dione (26). Following the procedure by which **19** was synthesized, treating 3-(2-cyanoethyl)pyrimidine-2,4-dione (**24**) (1.63 g, 9.85 mmol) in dry DMF (60 mL) with a 60% suspension of sodium hydride in mineral oil (0.39 g, 9.85 mmol) and then with (*R*)-3-(*t*-butoxycarbonylamino)oxetan-2-one (**47**) (1.84 g, 9.85 mmol) gave **26** (1.05 g, 39%) as a white solid: mp 210.8−211.7 °C (dec); $[\alpha]_D^{20} = +24$ (*c* 1.0, 6 M HCl); ee 99.9% as determined by chiral HPLC.

(*S*)-1-(2-Amino-2-carboxyethyl)-3-(2-carboxyethyl)-5-iodopyrimidine-2,4-dione (27). To a stirred suspension of (*S*)-1-(2-amino-2-carboxyethyl)-3-(2-carboxyethyl)-pyrimidine-2,4-dione (**25**) (0.3 g, 1.11 mmol) in a mixture of water (2.2 mL) and 2 M hydrochloric acid (2.2 mL) at room temperature was added 3 M iodine monochloride in 6 M hydrochloric acid (0.4 mL, 1.19 mmol). The mixture was heated to 70 °C for 1 h, a further aliquot of 3 M iodine monochloride in 6 M hydrochloric acid (0.4 mL, 1.19 mmol) was added, and the mixture was heated at 70 °C for 1 h. The solvent was then evaporated under reduced pressure. The residue was applied to a column of Dowex 50WX8-400 resin (0.25 mmol of cation/mL of resin; 10 mL). The column was eluted with water and then 1 M aqueous pyridine. The ninhydrin positive fractions of the 1 M aqueous pyridine eluate were combined and evaporated to dryness under reduced pressure. The solid was crystallized from water to give **27** (0.24 g, 55%) as a white solid: mp 210.9−212.0 °C (dec); $[\alpha]_D^{20} = +9.5$ (*c* 2.0, 6 M HCl); ee 98% as determined by chiral HPLC.

(*S*)-1-(2-Amino-2-carboxyethyl)-3-(2-carboxyethyl)-5-nitropyrimidine-2,4-dione (28). To a stirred suspension of (*S*)-1-(2-amino-2-carboxyethyl)-3-(2-carboxyethyl)-pyrimidine-2,4-dione (**25**) (0.2 g, 0.74 mmol) in concentrated sulfuric acid (2 mL) at 0 °C was added fuming nitric acid (0.12 mL) dropwise. Stirring was continued for 1 h at 0 °C and then at room temperature for 24 h. The mixture was poured onto ice, neutralized with solid sodium carbonate, and evaporated under reduced pressure. The residue was applied to a column of Dowex 50WX8-400 resin (0.25 mmol of cation/mL of resin; 100

mL). The column was eluted with water and then 1 M aqueous pyridine. The ninhydrin positive fractions of the 1 M aqueous pyridine eluate were combined and evaporated to dryness under reduced pressure. The solid was crystallized from water to give **28** (0.09 g, 36%) as brown crystals: mp 180.0−181.3 °C (dec); $[\alpha]_D^{20} = +8.8$ (*c* 1.36, 6 M HCl); ee 95% as determined by chiral HPLC.

3-(3-Cyanopropyl)-2-ethoxypyrimidin-4-one (29) and 4-(3-Cyanopropyloxy)-2-ethoxypyrimidine (31). The sodium salt of 2-ethoxy-4-ketopyrimidine (**12a**) (5.0 g, 31 mmol) was dissolved in dry DMF (80 mL) and heated to 60 °C under a dry nitrogen atmosphere. 4-Bromobutyronitrile (3.1 mL, 31 mmol) in dry DMF (30 mL) was added dropwise and the resulting mixture stirred at 60 °C for 48 h. The mixture was acidified with glacial acetic acid (3 mL) and the solvent removed under reduced pressure. The residue was flash chromatographed over silica gel. Elution with petroleum ether/ethyl acetate (40:60) gave **29** (2.9 g, 45%) and **31** (2.4 g, 37%) as yellow oils.

3-(3-Cyanopropyl)pyrimidine-2,4-dione (32). 3-(3-Cyanopropyl)-2-ethoxypyrimidin-4-one (**29**) (2.8 g, 14 mmol) was dissolved in concentrated hydrochloric acid/THF (200 mL, 1:10). After stirring for 20 h at room temperature, the solvent was evaporated under reduced pressure to give **32** (2.1 g, 84%) as a white solid: mp 140.0−140.7 °C.

(*S*)-1-(2-Amino-2-carboxyethyl)-3-(3-carboxypropyl)pyrimidine-2,4-dione (33). A 60% suspension of sodium hydride in mineral oil (0.13 g, 3.35 mmol) was added to a solution of 3-(3-cyanopropyl)pyrimidine-2,4-dione (**32**) (0.60 g, 3.35 mmol) in dry DMF (70 mL). After stirring for 5 h at room temperature, (*S*)−(3-(*t*-butoxycarbonyl)oxetan-2-one (**46**) (0.63 g, 3.35 mmol) was added. Stirring was continued for 72 h at room temperature, and then the mixture was evaporated under reduced pressure. The residue was dissolved in 6 M HCl and heated under reflux for 24 h. The mixture was evaporated under reduced pressure, and the residue was dissolved in water (10 mL) and applied to Dowex 50WX8-400 ion-exchange resin (H^+ form) (0.25 mmol of cation/mL of resin; 15 mL) with stirring for 30 min. The mixture was then applied to a column containing 20 mL of Dowex 50WX8-400 ion-exchange resin (H^+ form) and eluted with water followed by 1 M aqueous pyridine. The ninhydrin positive fractions of the 1 M aqueous pyridine eluate were combined and evaporated under reduced pressure. The residue was dissolved in water (10 mL) and applied to Biorad AG1X8 ion-exchange resin (acetate form) (0.5 mmol of anion/mL of resin; 10 mL) and stirred for 30 min. The mixture was then poured onto an equivalent volume of identical resin and eluted with increasing concentrations of acetic acid of 0.01, 0.1, and 0.5 M. The ninhydrin positive fractions of the 0.5 M acetic acid eluate were combined and concentrated under reduced pressure. Crystallization of the residue from water gave **33** as a white solid (0.28 g, 29%): mp 199.9−201.2 °C (dec); $[\alpha]_D^{20} = -22.0$ (*c* 1.0, 6 M HCl); ee 99% as determined by chiral HPLC.

(*R*)-1-(2-Amino-2-carboxyethyl)-3-(3-carboxypropyl)-pyrimidine-2,4-dione (34). Following the procedure by which **33** was synthesized, treating 3-(3-cyanopropyl)pyrimidine-2,4-dione (**32**) (1.02 g, 5.66 mmol) in dry DMF (40 mL) with a 60% suspension of sodium hydride in mineral oil (0.23 g, 5.66 mmol) and then with (*R*)-3-(*t*-butoxycarbonylamino)oxetan-2-one (**47**) (1.06 g, 5.66 mmol) gave **34** (0.33 g, 20%) as a white solid: mp 200.4−201.7 °C (dec); $[\alpha]_D^{20} = +21$ (*c* 1.0, 6 M HCl); ee 99.9% as determined by chiral HPLC.

Acid Hydrolysis of 4-(3-Cyanopropyloxy)-2-ethoxypyrimidine (31). 4-(3-Cyanopropyloxy)-2-ethoxypyrimidine (**31**) (2.4 g, 12 mmol) was dissolved in THF/concentrated hydrochloric acid (9:1) and heated under reflux for 2 h. It was then filtered to give **35** (1.1 g, 81%) as a white solid: mp 315.2−317.4 °C; lit. mp 330 °C.[35]

3-(2-Cyanobenzyl)pyrimidine-2,4-dione (37a). A solution of 2-(bromomethyl)benzonitrile (18.2 g, 92.5 mmol) in dry DMF (90 mL) was added dropwise to a stirred suspension of 2-ethoxypyrimidin-4-one sodium salt (**12a**) (15.0 g, 92.5 mmol) in dry DMF (240 mL) and stirred for 2 days at 60 °C under a dry nitrogen atmosphere. The solvent was removed at 50 °C under reduced pressure, and the products were separated from the insoluble salts by repeated washings with ethyl acetate (3 × 100 mL), which were subsequently combined, filtered, and evaporated under reduced pressure. The resulting mixture was purified using silica gel chromatography. Elution with petroleum ether/ethyl acetate (7:3) gave **36a** (5.3 g, 21%) as a crystalline solid: mp 110.7−111.1 °C.

3-(2-Cyanobenzyl)-2-ethoxypyrimidin-4-one (**36a**) (5.0 g, 19.6 mmol) was dissolved in concentrated hydrochloric acid/THF (1:10, 300 mL). After stirring for 20 h at room temperature, the mixture was concentrated under reduced pressure and the residue was crystallized from methanol (250 mL). The solid was filtered and washed with cold methanol (2 × 50 mL) to yield **37a** as a white solid (4.2 g, 93%): mp 216.2−218.2°C.

3-(3-Cyanobenzyl)pyrimidine-2,4-dione (37b). A solution of 3-(bromomethyl)benzonitrile (18.2 g, 92.5 mmol) in dry DMF (90 mL) was added dropwise to a stirred suspension of 2-ethoxypyrimidin-4-one sodium salt (**12a**) (15.0 g, 92.5 mmol) in dry DMF (240 mL) and stirred for 2 days at 60 °C under a dry nitrogen atmosphere. The solvent was removed at 50 °C under reduced pressure, and the products were separated from the insoluble salts by repeated washings with ethyl acetate (3 × 100 mL), which were subsequently combined, filtered, and evaporated under reduced pressure. The resulting mixture was purified using silica gel chromatography. Elution with petroleum ether/ethyl acetate (3:1) gave **36b** (9.2 g, 39%) as a crystalline solid: mp 102.6−103.2 °C.

3-(3-Cyanobenzyl)-2-ethoxypyrimidin-4-one (**36b**) (8.2 g, 32.1 mmol) was dissolved in THF/concentrated HCl (10:1, 216 mL). After stirring for 20 h at room temperature, the mixture was concentrated under reduced pressure and the residue was crystallized from ethyl acetate (500 mL). The solid was filtered and washed with cold ethyl acetate/petroleum ether (2 × 50 mL) to give **37b** (5.6 g, 77%) as a white solid: mp 186.9−187.9 °C.

3-(4-Cyanobenzyl)pyrimidine-2,4-dione (37c). The sodium salt of 2-ethoxypyrimidin-4-one (**12a**) (5.0 g, 31 mmol) was dissolved in dry DMF (80 mL) under a dry nitrogen atmosphere. A solution of 4-(bromomethyl)benzonitrile (6.05 g, 31 mmol) in dry DMF (30 mL) was added dropwise while the mixture was stirring at 60 °C. The mixture was stirred for 2 days at 60 °C. The solvent was removed under reduced pressure and the residue flash chromatographed over silica gel. Elution with petroleum ether/ethyl acetate (60:40) gave **36c** (3.9 g, 52%) as a white solid: mp 131.0−131.4 °C.

3-(4-Cyanobenzyl)-2-ethoxypyrimidin-4-one (**36c**) (3.8 g, 16 mmol) was dissolved in concentrated hydrochloric acid/THF (100 mL, 1:10). After stirring for 20 h at room temperature, the solvent was evaporated under reduced pressure and the residue crystallized from ethyl acetate to give **37c** (3.2 g, 91%) as a white solid: mp 230.0−231.8 °C.

***(RS)*-1-(2-Amino-2-carboxyethyl)-3-(2-carboxybenzyl)-pyrimidine-2,4-dione (38a).** A 60% suspension of sodium hydride in mineral oil (0.16 g, 4.0 mmol) was added portionwise to a stirred solution of 3-(2-cyanobenzyl)pyrimidine-2,4-dione (**37a**) (0.91 g, 4.0 mmol) in dry DMF (25 mL) and stirred for 2 h. (*S*)-3-(*t*-Butoxycarbonylamino)oxetan-2-one (**46**) (0.75 g, 4.0 mmol) was added portionwise and stirred at room temperature for 2 days. The mixture was evaporated under reduced pressure and the residue triturated with diethyl ether. The resulting white solid was dissolved in 6 M HCl (24 mL) and heated under reflux for 6 days. The mixture was evaporated under reduced pressure to leave a cream solid, which was dissolved in the minimum amount of water and applied to a column of Dowex 50WX8-400 ion-exchange resin (H^+ form) (0.25 mmol of cation/mL of resin; 5 mL). The column was eluted with water until no ninhydrin positive fractions were observed and then 1 M aqueous pyridine. The ninhydrin positive fractions of the 1 M aqueous pyridine eluate were combined and evaporated to dryness under reduced pressure. Crystallization of the residue from water yielded **38a** (0.78 g, 58%) as a white solid: mp 190.8−191.2 °C (dec); $[\alpha]_D^{20} = -2.0$ (*c* = 1.0, 6 M HCl); 12% ee as determined by chiral HPLC.

(*S*)-1-(2-Amino-2-carboxyethyl)-3-(3-carboxybenzyl)pyrimidine-2,4-dione (38b). A 60% suspension of sodium hydride in mineral oil (0.07 g, 1.8 mmol) was added portionwise to a stirred solution of 3-(3-cyanobenzyl)pyrimidine-2,4-dione (**37b**) (0.41 g, 1.8 mmol) in dry DMF (20 mL) and stirred for 2 h. (*S*)-3-(*t*-Butoxycarbonylamino)oxetan-2-one (**46**) (0.33 g, 1.8 mmol) was added portionwise and stirred at room temperature for 2 days. The mixture was evaporated under reduced pressure and the residue triturated with diethyl ether. The resulting white solid was dissolved in 6 M HCl (30 mL), and the solution was heated under reflux for 90 h. The mixture was evaporated under reduced pressure to leave a cream solid, which was dissolved in water and applied to a column of Dowex 50WX8-400 ion-exchange resin (H^+ form) (0.25 mmol of cation/mL of resin; 4 mL). The column was eluted with water until no ninhydrin positive fractions were observed and then 1 M aqueous pyridine. The ninhydrin positive fractions of the 1 M aqueous pyridine eluate were combined and evaporated to dryness under reduced pressure. The residue was dissolved in the minimum amount of water and bound to Biorad AG1X8 ion-exchange resin (acetate form) (0.5 mmol of anion/mL of resin; 5 mL) and poured onto an equivalent volume of identical resin. The column was eluted with water and then aqueous acetic acid of increasing concentrations of 0.01, 0.05, 0.1, 0.2, 0.25, and 0.3 M. The ninhydrin positive fractions of the 0.3 M acetic acid eluate were combined and evaporated under reduced pressure. Crystallization of the residue from boiling water yielded **38b** (0.12 g, 20%) as a white solid: mp 187.1−197.8 °C (dec); $[\alpha]_D^{20} = -11.0$ (*c* = 1.0, 6 M HCl);. 91% ee as determined by chiral HPLC.

(*S*)-1-(2-Amino-2-carboxyethyl)-3-(4-carboxybenzyl)pyrimidine-2,4-dione (38c). Following the procedure by which **38b** was synthesized, treating 3-(4-cyanobenzyl)pyrimidine-2,4-dione (**37c**) (1.84 g, 8.54 mmol) in dry DMF (60 mL) with a 60% suspension of sodium hydride in mineral oil (0.34 g, 8.54 mmol) and then with (*S*)-3-(*t*-butoxycarbonylamino)-oxetan-2-one (**46**) (1.59 g, 8.54 mmol) gave an intermediate that was suspended in 6 M hydrochloric acid (60 mL) and heated under reflux for 2 h. Purification by ion-exchange chromatography following the procedure for **38b** gave **38c** (0.52 g, 20%) as a white solid: mp 215.8−216.4 °C (dec); $[\alpha]_D^{20} = -28.7$ (*c* 0.5, 6 M HCl); 96% ee as determined by chiral HPLC.

(*S*)-1-(2-Amino-2-carboxyethyl)-3-(4-carboxybenzyl)-5-iodopyrimidine-2,4-dione (39). To a solution of (*S*)-1-(2-amino-2-carboxyethyl)-3-(4-carboxybenzyl)pyrimidine-2,4-dione (**38c**) (0.40 g, 1.1 mmol) in 1 M aqueous hydrochloric acid (3 mL) was added a solution of iodine monochloride (0.23 g, 1.4 mmol) in 6 M aqueous hydrochloric acid (0.5 mL). After stirring at 70 °C for 20 h, a further equivalent of iodine monochloride (0.23 g, 1.4 mmol) in 6 M aqueous hydrochloric acid (0.5 mL) was added. Stirring was continued for 20 h, and then the solvent was removed under reduced pressure and the resulting white solid was applied as a slurry in water (5 mL) to a column of Dowex 50WX8-400 ion-exchange resin (H^+ form) (20 mL). The column was washed with water and eluted with 1 M aqueous pyridine. The ninhydrin positive fractions of the 1 M pyridine eluate were combined and evaporated to dryness under reduced pressure. The resulting residue was crystallized from water with exclusion of sunlight to give **39** (0.24 g, 41%) as a white solid: mp 214.1−214.4 °C; $[\alpha]_D^{20} = +10.0$ (*c* 1.0, 6 M HCl); >99% ee as determined by chiral HPLC.

(*S*)-3-[3-(2-Amino-2-carboxyethyl)ureidomethyl]benzoic Acid (40). A 60% suspension of sodium hydride in mineral oil (0.26 g, 6.6 mmol) was added portionwise to a stirred solution of 3-(3-cyanobenzyl)pyrimidine-2,4-dione (**37b**) (1.50 g, 6.6 mmol) in dry DMF (50 mL) and stirred for 20 min. (*S*)-3-(*t*-Butoxycarbonylamino)oxetan-2-one (**46**) (1.24 g, 6.6 mmol) was added portionwise and stirred at room temperature for 2 days. The mixture was evaporated under reduced pressure to leave a white solid. To this was added 6 M HCl (100 mL), and the solution was heated under reflux for 4.5 h. The mixture was evaporated under reduced pressure to leave a white powder, which was dissolved in the minimum amount of water and applied to a column of Dowex 50WX-400 ion-exchange resin (H^+ form) (0.25 mmol of cation/mL of resin; 50 mL). The column was eluted with water and then 1 M aqueous pyridine. The ninhydrin positive fractions of the 1 M aqueous pyridine eluate were combined and evaporated to dryness under reduced pressure. The residue was dissolved in the minimum amount of water and bound to Dowex X18-400 ion-exchange resin (hydroxide form) adding the resin until the amino acid was undetectable by TLC in the supernatant. The resulting resin was applied to an equivalent amount of Dowex X18-400 ion-exchange resin (acetate form). The column was eluted with water and then aqueous acetic acid of increasing concentrations of 0.01, 0.05, 0.1, and 0.3 M. The ninhydrin positive fractions of the 0.3 M aqueous acetic acid eluate were combined and evaporated under reduced pressure. Crystallization of the residue from water yielded **40** (0.9 g, 47%) as a white solid: mp 209.8−210.9 °C; $[\alpha]_D^{23} = -40.0°$ (*c* 0.1, 6 M HCl); 98% ee as determined by chiral HPLC.

2-Ethoxy-3-(2-methoxycarbonylbenzyl)pyrimidin-4-one (41). A solution of methyl 2-bromomethylbenzoate (33.1 g, 123 mmol) in dry DMF (200 mL) was added to the monosodium salt of 2-ethoxypyrimidin-4-one (**12a**) (20 g, 123 mmol) under a dry nitrogen atmosphere. The mixture was stirred at 60 °C for 2 days under a dry nitrogen atmosphere. The solvent was removed at 60 °C under reduced pressure to give a brown oil, which was taken up in water (100 mL) and extracted with ethyl acetate (3 × 100 mL). The extracts were combined, washed once with brine (50 mL), dried ($MgSO_4$), filtered, and evaporated under reduced pressure. The resulting mixture was purified using silica gel chromatography and eluted with petroleum ether/ethyl acetate [gradient elution (7:3)−(3:7)]. This gave **41** (2.0 g, 6%) as a crystalline solid: mp 93.6−95.6 °C.

3-(2-Carboxybenzyl)pyrimidine-2,4-dione (43). 2-Ethoxy-3-(2-methoxycarbonylbenzyl)pyrimidin-4-one **(41)** (1.2 g, 4.3 mmol) was dissolved in acetonitrile/6 M HCl (10:1, 30 mL). After stirring for 20 h at room temperature, the mixture was concentrated under reduced pressure. The residue was crystallized from methanol to give 3-(2-methoxycarbonylbenzyl)-pyrimidine-2,4-dione (**42**) (1.1 g, 99%) as white prisms: mp 221.5−223.5 °C.

3-(2-Methoxycarbonylbenzyl)pyrimidine-2,4-dione (**42**) (1.0 g, 3.85 mmol) was suspended in ethanol (50 mL), and a solution of sodium hydroxide (0.3 g, 7.70 mmol) in water (20 mL) was added. The mixture was heated under reflux for 3 days. The mixture was acidified with 1 M HCl and the white precipitate collected by filtration. The resulting solid was washed with water and ethanol and crystallized from ethanol and then from water to give **43** (0.84 g, 89%) as a white solid: mp 279.5−280.5 °C.

(*S*)-1-(2-Amino-2-carboxyethyl)-3-(2-carboxybenzyl)pyrimidine-2,4-dione (44a). A 60% suspension of sodium hydride in mineral oil (0.27 g, 6.8 mmol) was added portionwise to a stirred solution of 3-(2-carboxybenzyl)pyrimidine-2,4-dione (**43**) (0.84 g, 3.4 mmol) in dry DMF (20 mL) and stirred for 1 h. (*S*)-3-(*t*-Butoxycarbonylamino)oxetan-2-one (**46**) (0.64 g, 3.4 mmol) was added portionwise and stirred at room temperature for 2 days. The mixture was evaporated under reduced pressure, and the resulting residue was dissolved in 2 M HCl and evaporated under reduced pressure to leave a white solid. The resulting white solid was suspended in water (10 mL) and applied to Dowex 50WX8-400 ion-exchange resin (H^+ form) (0.25 mmol of cation/mL of resin; 50 mL) with stirring for 30 min. The mixture was then applied to a column containing 40 mL of Dowex 50WX8-400 ion-exchange resin (H^+ form) and eluted with water until no ninhydrin positive fractions were observed, THF/water (1:1) until the eluate was colorless, and then 1 M aqueous pyridine. The ninhydrin positive fractions of the 1 M aqueous pyridine eluate were combined and evaporated to dryness under reduced pressure. The residue was suspended in water (10 mL) and bound to Biorad AG1X8 ion-exchange resin (acetate form) (0.5 mmol of anion/mL of resin; 20 mL) and poured onto an equivalent volume of the same resin. The column was then eluted with water and then aqueous acetic acid of increasing concentra-

tions of 0.01, 0.1, 0.5, 1.0, and 2.0 M. The ninhydrin positive fractions of the 2.0 M acetic acid eluate were combined and evaporated under reduced pressure. Crystallization of the residue from water yielded **44a** (0.75 g, 66%) as a white solid: mp 207.9−208.5 °C (dec); $[\alpha]_D^{20} = -12.0$ (*c* 1.0., 6 M HCl); ee > 99% as determined by chiral HPLC.

(*R*)-1-(2-Amino-2-carboxyethyl)-3-(2-carboxybenzyl)-pyrimidine-2,4-dione (44b). Following the procedure by which **44a** was synthesized, treating 3-(2-carboxybenzyl)-pyrimidine-2,4-dione (**43**) (0.80 g, 3.3 mmol) in dry DMF (20 mL) with a 60% suspension of sodium hydride in mineral oil (0.26 g, 6.5 mmol) and then with (*R*)-3-(*t*-butoxycarbonylamino)oxetan-2-one (**47**) (0.61 g, 3.3 mmol) gave **44b** (0.65 g, 60%) as a white solid: mp 205.5−207.2 °C (dec); $[\alpha]_D^{20} = +15.7$ (*c* 0.37, 6 M HCl); ee >98% as determined by chiral HPLC.

(*S*)-1-(2-Amino-2-carboxyethyl)-3-(2-carboxybenzyl)-5-iodo-pyrimidine-2,4-dione (45). To a solution of (*S*)-1-(2-amino-2-carboxyethyl)-3-(2-carboxybenzyl)pyrimidine-2,4-dione (**44a**) (0.30 g, 0.9 mmol) in 1 M aqueous hydrochloric acid (10 mL) was added a solution of iodine monochloride (0.29 g, 1.7 mmol) in 6 M aqueous hydrochloric acid (0.6 mL). The mixture was stirred at 70 °C for 7 h. A further equivalent of iodine monochloride (0.29 g, 1.7 mmol) in 6 M aqueous hydrochloric acid (0.6 mL) was then added. After stirring for 20 h at 70 °C, the solvent was removed under reduced pressure and the resulting white solid was applied as a slurry in water (10 mL) to Dowex 50WX8-400 ion-exchange resin (H^+ form) (20 mL) and stirred for 30 min. The mixture was applied to a column containing Dowex 50WX8-400 ion-exchange resin (H^+ form) (20 mL) and eluted with water, THF/water (1:1), and then 1 M aqueous pyridine. The ninhydrin positive fractions of the 1 M pyridine eluate were combined and evaporated to dryness under reduced pressure. The residue was crystallized from water with exclusion of sunlight to give **45** (0.24 g, 41%) as a white solid: mp 206.1−207.0 °C (dec); $[\alpha]_D^{20} = +12.0$ (*c* = 0.5, 6 M HCl); ee >99% as determined by chiral HPLC.

Electrophysiology. Reduction of the fDR-VRP by AMPA Receptor Antagonists. Hemisected spinal cords from nonanesthetized 1- to 5-day old rats killed by cervical dislocation were prepared and used according to the reported method.[36] To assess AMPA receptor antagonist activity the ability of the compounds to block the fast component of the dorsal root evoked ventral root potential (fDR-VRP) in the neonatal rat hemisected spinal cord preparation was measured, as described in detail previously.[11] Concentration response curves were constructed for test antagonists (5 min applications), in the presence of 2 mM $MgSO_4$/50 μM (*R*)-2-amino-5-phosphonopentanoic acid (*R*)-AP5 (30 min preincubation) to block NMDA receptors. Results are expressed as mean ± SEM, $n = 3$. Throughout experiments used to measure the fDR-VRP, a slow trace was also recorded which showed dc shifts in ventral root potential. Depolarizations observed on this trace indicated that the test compound had agonist activity.

Antagonism of Kainate Responses on Dorsal Root C-Fibers by Novel Willardiine Derivatives. Experiments to test the antagonistic effect of the novel compounds at GLU_{K5}-containing kainate receptors were conveniently carried out on kainate-induced responses on isolated neonatal rat dorsal roots, as described in detail previously.[11] To prevent desensitization of kainate receptors, the dorsal root was superfused with 1 mg mL^{-1} concanavalin A[40] for 20 min after a 20 min exposure to glucose-free superfusion medium. Standard superfusion medium was then applied throughout the experiments. This allowed measurement of depolarizations evoked by the exogenously applied agonist, kainate (1 min applications). Noncumulative, nonsequential concentration−response curves were constructed for kainate in the absence and presence of the antagonist (30 min preincubation).

Electrophysiology in Hippocampal Slice. Extracellular fEPSPs were recorded in the CA3 region of hippocampal slices as described previously.[11] EPSPs were evoked by low-frequency stimulation of the mossy fiber pathway via an electrode placed in the dentate gyrus. A mossy fiber LTP study was carried out in slices from 6- to 10-week-old rats, with LTP induced by delivering 100 shocks at 100 Hz at test intensity, in the presence of the NMDA receptor antagonist (*R*)-AP5.

Native AMPA and Kainate Receptor Binding Assays. Cerebellum-free brain membrane preparations were made from male Wistar rats (250−300 g). Binding assays were performed using 0.4 mg/mL protein, increasing concentrations of novel compound, and either 10 nM [^{3}H]-**9** or 5 nM [^{3}H]-SYM2081 ([^{3}H]-**48**), depending on whether selectivity for AMPA or kainate receptors was being studied. Mixtures were incubated at 4 °C for 40 min. Nonspecific binding was defined in the presence of 1 mM (*S*)-glutamate. Unbound radioligand was removed by washing with assay buffer (50 mM Tris HCl/100 mM KCl, pH 7.4) using a Brandell cell harvester. Bound ligand was assessed using a Wallac scintillation counter. Concentration−inhibition curves for each compound were constructed in GraphPad Prism and IC_{50} values derived. K_i values were calculated using the Cheng−Prussoff equation.

Recombinantly Expressed Rat GLU_{K6} Kainate Receptor Binding Assay in HEK293 Cells. For radioligand binding studies, HEK293 cells were transfected with GLU_{K6} DNA using Lipofectamine 2000 and then membranes harvested 2 days later as described in detail previously.[11] Displacement radioligand binding studies were carried out in the presence of 10 nM [^{3}H]kainate, with nonspecific binding defined as that not displaced by 100 μM kainate. The novel compounds were tested at concentrations of 10 μM, 100 μM, and 1 mM to give an initial indication of their affinity. Competition binding curves were generated for the standard kainate receptor ligands (*S*)-glutamate (**1**) and **46** and analyzed by iterative nonlinear regression using GraphPAD Prism.[11]

[^{3}H]Kainate Displacement Assay for GLU_{K7}. Membrane Preparation. Adherent HEK293 cells stably transfected with human GLU_{K7} kainate receptors were thawed and lysed in 10 volumes of ice cold distilled water and centrifuged for 30 min at 40000*g*. The resulting pellets were resuspended in >100 volumes of assay buffer (50 mM Tris-HCl, pH 7.4) and centrifuged at 40000*g* again to remove endogenous glutamate. The resulting pellets were resuspended in 4 mL assay buffer and subjected to [^{3}H]kainate binding experiments.

[^{3}H]Kainate Displacement Assay. Inhibition of [^{3}H]-kainate binding by **38a** or **47** was carried out in borosilicate tubes containing 125 μg of membrane protein, 7 nM [^{3}H]-kainate (PerkinElmer, Boston, MA), test compounds in a range of concentrations, and assay buffer to a final volume of 200 μL. Nonspecific binding was defined by 10 mM glutamate (**1**). Incubation was carried out at 4 °C for 2 h and terminated by rapid filtration (Millipore 12 port vacuum manifold) through Whatman GF/B filters presoaked in 0.03% polyethylenimine. Filters were washed 3 times with 2 mL of cold assay buffer, and the retained radioactivity on the filters was measured using a liquid scintillation counter (Beckman LS6000TA instrument). Protein was determined by BCA method (Pierce, Rockford, IL). Competition binding curves were analyzed using GraphPad Prism 3.02 (San Diego, CA) with slope factor set at 1 and top and bottom fixed at 100% and 0% of control [^{3}H]-kainate binding, respectively. The dissociation constant (K_i) for test compounds was calculated according to the Cheng−Prusoff equation.

[^{3}H]Kainate binds to membranes from these cells with $K_D = 5.3 \pm 0.8$ nM and $B_{max} = 3.0 \pm 0.1$ pmol/mg, determined from saturation binding experiments performed under the same conditions.

Calcium Fluorescence Assays Using Recombinant Human AMPA and Kainate Receptor Subtypes. AMPA Receptor Assays. HEK293 cells stably expressing human AMPA receptors were seeded into poly-D-lysine-coated 96-well plates (Becton Dickinson Labware, Bedford, MA) 1 or 2 days prior to experiments at 60 000 cells/well (1 day) or 30 000 cells/well (2 day). Cells were washed 3 times with 100 μL of assay buffer composed of Hanks balanced salt solution without phenol red (Invitrogen) with 20 mM HEPES and 3.7 mM $CaCl_2$ added (final $[CaCl_2] = 5$ mM). Plates were then incubated for 2−3 h at room temperature in 40 μL of assay buffer with 8

μM Fluo3-AM dye (Molecular Probes Inc., Eugene, OR). Following dye incubation, cells were rinsed once with 100 μL of assay buffer. Finally, 50 μL of assay buffer, which included the AMPA receptor potentiator LY392098 (10 μM; to prevent desensitization of AMPA receptors), was added to wells and fluorescence measured using a fluorometric imaging plate reader (FLIPR; Molecular Devices, Sunnyvale, CA). The FLIPR added a first addition of 50 μL of LY392098-containing assay buffer, followed by a second addition of 100 μL of LY392098-containing buffer 3 min later. **38a** was added in the absence of agonist during the first addition, and in the presence of 100 μM glutamate (**1**) during the second addition.

Kainate Receptor Assays. All receptor clones were stably expressed in HEK293 cells. The GLU_{K5}(Q)/GLU_{K2} cell line was created by retroviral infection of cDNA coding for the human GLU_{K2} subunit (EAA2; Allelix Biopharmaceuticals) into the GLU_{K5}(Q)-expressing cell line using the pMNLZRS/IB retroviral expression vector. HEK293 cell lines stably expressing a cloned GLU_{K5}(Q)[37] or GLU_{K6}(Q) receptor subunit,[38] or coexpressing GLU_{K5}(R) and GLU_{K6}(Q),[4c] or GLU_{K6}(Q) and GLU_{K2}[39] have been previously described. Kainate receptor expression levels for all transfected cell lines have been previously determined by saturation binding of [^{3}H]kainate to intact cells. B_{max} values for specific [^{3}H]kainate binding are as follows: GLU_{K5}(Q), 1.7 $\pm$ 0.5 pmol/mg; GLU_{K5}(R)/6(Q), 8 $\pm$ 2 pmol/mg; GLU_{K5}(Q)/GLU_{K2}, 0.6 $\pm$ 0.1 pmol/mg; GLU_{K6}(Q), 2.7 $\pm$ 0.3 pmol/mg; GLU_{K6}(Q)/GLU_{K2}, 1.7 $\pm$ 0.3 pmol/mg.[42]

Cell growth and ion influx studies using a fluorometric imaging plate reader (FLIPR; Molecular Devices, Sunnydale, CA) were carried out exactly as described previously, in the presence of concanavalin A.[11] The antagonist **38a** was added in the absence of agonist during the first addition, and in the presence of 100 μM glutamate during the second addition. Concentration−response curves for **38a** were analyzed using GraphPad Prism 3.02 software (San Diego, CA), with slope factor fixed at 1, and top and bottom fixed at 100% and 0% inhibition, respectively. The dissociation constant (K_b) was calculated from the IC_{50} value for inhibiting 100 μM glutamate-induced calcium influx according to the Cheng−Prusoff equation:[41]

$$K_b = IC_{50}/(1 + [Glu]/EC_{50\ Glu})$$

where [Glu] is the concentration of glutamate (**1**) (100 μM) and $EC_{50\ Glu}$ is the EC_{50} value of glutamate for evoking calcium influx in the given cell line, determined from glutamate concentration−response curves run in the same plate as **38a** concentration−response curves.

Acknowledgment. We would like to thank the BBSRC, the MRC, the EPSRC, and Tocris Cookson Ltd. for sponsoring this work.

Supporting Information Available: Spectroscopic data and elemental analyses for intermediates and final compounds. This material is available free of charge via the Internet at http://pubs.acs.org.

References

(1) (a) Watkins, J. C.; Krogsgaard-Larsen, P.; Honoré, T. Structure-activity relationships in the development of excitatory amino acid receptor agonists and competitive antagonists. *Trends Pharmacol. Sci.* **1990**, *11*, 25−33. (b) Jane, D. E. Antagonists acting at the NMDA receptor complex: potential for therapeutic applications. In *Glutamate and GABA receptors and transporters*; Krogsgaard-Larsen, P., Egebjerg, J., Schousboe, A., Eds.; Taylor and Francis: London, 2002; pp 69−98. (c) Schoepp, D. D.; Jane, D. E.; Monn, J. A. Pharmacological agents acting at subtypes of metabotropic glutamate receptors. *Neuropharmacology* **1999**, *38*, 1431−1476.

(2) (a) Fletcher, E. J.; Lodge, D. New developments in the molecular pharmacology of α-amino-3-hydroxy-5-methyl-4-isoxazolepropionate and kainate receptors. *Pharmacol. Ther.* **1996**, *70*, 65−89. (b) Bleakman, D.; Lodge, D. Neuropharmacology of AMPA and kainate receptors. *Neuropharmacology* **1998**, *37*, 1187−1204. (c) Jane, D. E.; Tse, H.-W.; Skifter, D. A.; Christie, J. M.; Monaghan, D. T. Glutamate receptor ion channels: Activators and inhibitors. In *Pharmacology of Ionic Channel Function: Activators and Inhibitors*; Endo, M., Kurachi Y., Mishina, M., Eds.; Springer-Verlag: Berlin, 2000; pp 415−459.

(3) (a) Bettler, B.; Mulle, C. Neurotransmitter receptors. 2. AMPA and kainate receptors. *Neuropharmacology* **1995**, *34*, 123−139. (b) Chittajallu, R.; Braithwaite, S. P.; Clarke, V. R.; Henley, J. M. Kainate receptors: subunits, synaptic localization and function. *Trends Pharmacol. Sci.* **1999**, *20*, 26−35. (c) Lodge, D.; Dingledine, R. *Ionotropic Glutamate Receptors. The IUPHAR Compendium of Receptor Characterization and Classification*, 2nd ed.; IUPHAR Media Ltd: London, 2001.

(4) (a) Clarke, V. R.; Ballyk, B. A.; Hoo, K. H.; Mandelzys, A.; Pellizzari, A.; Bath, C. P.; Thomas, J.; Sharpe, E. F.; Davies, C. H.; Ornstein, P. L.; Schoepp, D. D.; Kamboj, R. K.; Collingridge, G. L.; Lodge, D.; Bleakman, D.. A hippocampal GluR5 kainate receptor regulating inhibitory synaptic transmission. *Nature* **1997**, *389*, 599−603. (b) Vignes, M.; Clarke, V. R.; Parry, M. J.; Bleakman, D.; Lodge, D.; Ornstein, P. L.; Collingridge, G. L. The GluR5 subtype of kainate receptor regulates excitatory synaptic transmission in areas CA1 and CA3 of the rat hippocampus. *Neuropharmacology* **1998**, *37*, 1269−1277. (c) Bortolotto, Z. A.; Clarke, V. R.; Delany, C. M.; Parry, M. C.; Smolders, I.; Vignes, M.; Ho, K. H.; Miu, P.; Brinton, B. T.; Fantaske, R.; Ogden, A.; Gates, M.; Ornstein, P. L.; Lodge, D.; Bleakman, D.; Collingridge, G. L. Kainate receptors are involved in synaptic plasticity. *Nature* **1999**, *402*, 297−301. (d) Filla, S. A.; Winter, M. A.; Johnson, K. W.; Bleakman, D.; Bell, M. G.; Bleisch, T. J.; Castano, A. M.; Clemens-Smith, A.; Del Prado, M.; Dieckman, D. K.; Dominguez, E.; Escribano, A.; Ho, K. H.; Hudziak, K. J.; Katofiasc, M. A.; Martinez-Perez, J. A.; Mateo, A.; Mathes, B. M.; Mattiuz, E. L.; Ogden, A. M. L.; Phebus, L. A.; Stack, D. R.; Stratford, R. E.; Ornstein, P. L. Ethyl (3*S*,4a*R*,6*S*,8a*R*)-6-(4-ethoxycarbonylimidazol-1-ylmethyl)decahydroisoquinoline-3-carboxylic ester: a prodrug of a GluR5 kainate receptor antagonist active in two animal models of acute migraine. *J. Med. Chem.* **2002**, *45*, 4383−4386.

(5) (a) O'Neill, M. J.; Bond, A.; Ornstein, P. L.; Ward, M. A.; Hicks, C. A.; Hoo, K.; Bleakman, D.; Logde, D. Decahydroisoquinolines: novel competitive AMPA/kainate antagonists with neuroprotective effects in global cerebral ischaemia. *Neuropharmacology* **1998**, *37*, 1211−1222. (b) Simmons, R. M. A.; Li, D. L.; Hoo, K. H.; Deverill, M.; Ornstein, P. L.; Iyengar, S. Kainate GluR5 receptor mediates the nociceptive response to formalin in the rat. *Neuropharmacology* **1998**, *37*, 25−36. (c) O'Neill, M. J.; Bogaert, L.; Hicks, C. A.; Bond, A.; Ward, M. A.; Ebinger, G.; Ornstein, P. L.; Michotte, Y.; Lodge, D. LY377770, a novel iGluR5 kainate receptor antagonist with neuroprotective effects in global and focal cerebral ischaemia. *Neuropharmacology* **2000**, *39*, 1575−1588. (d) Smolders, I.; Bortolotto, Z. A.; Clarke, V. R. J.; Warre, R.; Khan, G. M.; O'Neill, M. J.; Ornstein, P. L.; Bleakman, D.; Ogden, A.; Weiss, B.; Stables, J. P.; Ho, K. H.; Ebinger, G.; Collingridge, G. L.; Lodge, D.; Michotte, Y. Antagonists of GLU_{K5}-containing kainate receptors prevent pilocarpine-induced limbic seizures. *Nat. Neurosci.* **2002**, *5*, 796−804.

(6) (a) Christensen, J. K.; Varming, T.; Ahring, P. K.; Jørgensen, T. D.; Nielsen, E. Ø. In vitro characterization of 5-carboxyl-2,4-dibenzamidobenzoic Acid (NS3763), a noncompetitive antagonist of GLU_{K5} receptors. *J. Pharmacol. Exp. Ther.* **2004**, *309*, 1003−1010. (b) Valgeirsson, J.; Nielsen, E. Ø.; Peters, D.; Kristensen, A. S.; Madsen, U. Bioisosteric Modifications of 2-arylureidobenzoic acids: selective noncompetitive antagonists for the homomeric kainate receptor subtype GluR5. *J. Med. Chem.* **2004**, *47*, 6948−6957.

(7) (a) Jane, D. E.; Pook, P. C.-K.; Sunter, D. C.; Udvarhelyi, P. M.; Watkins, J. C. New willardiine analogs with potent stereoselective actions on mammalian spinal neurones. *Br. Pharmacol.* **1991**, *104*, 333P. (b) Blake, J. F.; Jane, D. E.; Watkins, J. C. Action of willardiine analogs on immature rat dorsal roots. *Br. J. Pharmacol.* **1991**, *104*, 334P. (c) Patneau, D. K.; Mayer, M. L.; Jane, D. E.; Watkins, J. C. Activation and desensitization of AMPA/kainate receptors by novel derivatives of willardiine. *J. Neurosci.* **1992**, *12*, 595−606. (d) Wong, L. A.; Mayer, M. L.; Jane, D. E.; Watkins, J. C. Willardiines differentiate agonist binding sites for kainate-versus AMPA-preferring glutamate receptors in DRG and hippocampal neurones. *J. Neurosci.* **1994**, *14*, 3881−3897. (e) Hawkins, L. M.; Beaver, K. M.; Jane, D. E.; Taylor, P. M.; Sunter, D. C.; Roberts, P. J. Binding of the new radioligand (*S*)-[3H]-AMPA to rat-brain synaptic membranes—effects of a series of structural analogs of the non-NMDA receptor agonist willardiine. *Neuropharmacology* **1995**, *34*, 405−410. (f) Hawkins, L. M.; Beaver, K. M.; Jane, D. E.; Taylor, P. M.; Sunter, D. C.; Roberts, P. J. Characterization of the pharmacology and regional distribution of (*S*)-[3H]-5-fluorowillardiine binding in rat brain. *Br. J. Pharmacol.* **1995**, *116*, 2033−2039. (g) Hawkins, L. M.; Jane, D. E.; Roberts, P. J. The effect of 6-aza substitution on the affinity of willardiine derivatives for the AMPA receptor.

Br. J. Pharmacol. Proc. Suppl. **1995**, *117*, 332P. (h) Thompson, G. A.; Jane, D. E.; Watkins, J. C. Depolarising effects of certain derivatives of (*S*)-willardiine upon *in vitro* neonatal rat dorsal roots. *Br. J. Pharmacol. Proc. Suppl.* **1995**, *117*, 331P.

(8) Jane, D. E.; Hoo, K.; Kamboj, R.; Deverill, M.; Bleakman, D.; Mandelzys, A. Synthesis of Willardiine and 6-Azawillardiine analogs: Pharmacological characterization on cloned homomeric human AMPA and kainate receptor subtypes. *J. Med. Chem.* **1997**, *40*, 3645−3650.

(9) Madsen, U.; Bang-Andersen, B.; Brehm, L.; Christensen, I. T.; Ebert, B.; Kristoffersen, Y. L.; Krogsgaard-Larsen, P. Synthesis and pharmacology of highly selective carboxy and phosphono isoxazole amino acid AMPA receptor antagonists. *J. Med. Chem.* **1996**, *39*, 1682−1691.

(10) (a) Ornstein, P. L.; Arnold, M. B.; Augenstein, N. K.; Lodge, D.; Leander, J. D.; Schoepp, D. D. (3*SR*,4a*RS*,6*RS*,8a*RS*)-6-[2(1*H*Tetrazol-5-yl)ethyl]decahydroisoquinoline-3-carboxylic Acid: A Structurally novel, systemically active, competitive AMPA receptor antagonist. *J. Med. Chem.* **1993**, *36*, 2046−2048. (b) Ornstein, P. L.; Arnold, M. B.; Allen, N. K.; Bleisch, T.; Borromeo, P. S.; Lugar, C. W.; Leander, J. D.; Lodge, D.; Schoepp, D. D. Structure-activity studies of 6-(tetrazolylalkyl)-substituted decahydroisoquinoline-3-carboxylic acid AMPA receptor antagonists. 1. Effects of stereochemistry, chain length, and chain substitution. *J. Med. Chem.* **1996**, *39*, 2219−2231. (c) Ornstein, P. L.; Arnold, M. B.; Allen, N. K.; Bleisch, T.; Borromeo, P. S.; Lugar, C. W.; Leander, J. D.; Lodge, D.; Schoepp, D. D. Structure-activity studies of 6-substituted decahydroisoquinoline-3-carboxylic Acid AMPA receptor antagonists. 2. Effects of distal acid bioisosteric substitution, absolute stereochemical preferences, and in vivo activity. *J. Med. Chem.* **1996**, *39*, 2232−2244.

(11) (a) More, J. C. A.; Troop, H. M.; Jane, D. E. The novel antagonist 3-CBW discriminates between kainate receptors expressed on neonatal rat motoneurones and those on dorsal root C-fibres. *Br. J. Pharmacol.* **2002**, *137*, 1125−1133. (b) More, J. C. A.; Troop, H. M.; Dolman, N. P.; Jane, D. E. Structural requirements for novel willardiine derivatives acting as AMPA and kainate receptor antagonists. *Br. J. Pharmacol.* **2003**, *138*, 1093−1100. (c) More, J. C. A.; Nistico, R.; Dolman, N. P.; Clarke, V. R. J.; Alt, A. J.; Ogden, A. M.; Buelens, F. P.; Troop, H. M.; Kelland, E. E.; Pilato, F.; Bleakman, D.; Bortolotto, Z. A.; Collingridge, G. L.; Jane, D. E. Characterisation of UBP296; a novel, potent and selective kainate receptor antagonist. *Neuropharmacology* **2004**, *47*, 46−64.

(12) Hilbert, G. E.; Jansen, E. F. Action of alkali on 2,4-diethoxypyrimidine and the application of the reaction to a new synthesis of cytosine. *J. Am. Chem. Soc*. **1935**, *57*, 552−554.

(13) Nollet, A. J. H.; Pandit, U. K. Unconventional nucleotide analogues-III. 4-(N^1-pyrimidyl)-2-aminobutyric Acids. *Tetrahedron* **1968**, *25*, 5989−5994.

(14) (a) Arnold, L. D.; Drover, J. C. G.; Vederas, J. C. Conversion of serine beta-lactones to chiral alpha amino acids by copper-containing organolithium and organomagnesium reagents. *J. Am. Chem. Soc.* **1987**, *109*, 4649−4659. (b) Arnold, L. D.; Kalantar, T. H.; Vederas, J. C. Conversion of serine to stereochemically pure β-substituted α-amino acids via β-lactones. *J. Am. Chem. Soc*. **1985**, *107*, 7105−7109. (c) Ramer, S. E.; Moore, R. N.; Vederas, J. C. Mechanism of formation of serine β-lactones by Mitsunobu cyclization: synthesis and use of L-serine stereospecifically labelled with deuterium at C-3. *Can. J. Chem*. **1986**, *64*, 706−713.

(15) Novacek, A.; Lissnerova, M. Nucleic acid components and their analogues. CVII. Cyanoethylation of uracil and 2-thiouracil derivatives. *Collect. Czech. Chem. Commun*. **1968**, *33*, 604−609.

(16) Robins, M. J.; Barr, P. J.; Giziewicz, J. Nucleic acid related compounds. 38. Smooth and high yield iodination and chlorination at C-5 of uracil bases and p-tolyl-protected nucleosides. *J. Can. Chem.* **1982**, *60*, 554−557.

(17) Agrawal, S. G.; Evans, R. H. The primary afferent depolarizing action of kainate in the rat. *Br. J. Pharmacol.* **1986**, *87*, 345−355.

(18) (a) Bettler, B.; Boulter, J.; Hermans-Borgmeyer, I.; O'Shea-Greenfield, A.; Deneris, E. S.; Moll, C.; Borgmeyer, U.; Hollman, M.; Heinemann, S. Cloning of a novel glutamate receptor subunit, GluR5: expression in the central nervous system during development. *Neuron* **1990**, *5*, 583−595. (b) Wilding, T. J.; Huettner, J. E. Functional diversity and developmental changes in rat neuronal kainate receptors. *J. Physiol*. **2001**, *532.2*, 411−421. (c) Kerchner, G. A.; Wilding, T. J., Huettner, J. E.; Zhuo, M. Kainate receptor subunits underlying presynaptic regulation of transmitter release in the dorsal horn. *J. Neurosci.* **2002**, *22*, 8010−8017.

(19) Hawkins, L. M.; Beaver, K. M.; Jane, D. E.; Taylor, P. M.; Sunter, D. C.; Roberts, P. J. Characterization of the pharmacology and regional distribution of (S)-[^{3}H]-5-fluorowillardiine binding in rat brain. *Br. J. Pharmacol*. **1995**, *116*, 2033−2039.

(20) Toms, N. J.; Reid, M. E.; Phillips, W.; Kemp, M. C.; Roberts, P. J. A novel kainate receptor ligand [^{3}H]-(2S,4R)-4-methylglutamate: pharmacological characterization in rabbit brain membranes. *Neuropharmacology* **1997**, *36*, 1483−1488.

(21) (a) Lomeli, H.; Wisden, W.; Kohler, M.; Keinanen, K.; Sommer, B.; Seeburg, P. H. High-affinity kainate and domoate receptors in rat brain. *FEBS Lett.* **1992**, *307*, 139−143. (b) Swanson, G. T., Gereau, R. W.; Green, T.; Heinemann, S. F. Identification of amino acid residues that control functional behavior in GluR5 and GluR6 kainate receptors. *Neuron* **1997**, *19*, 913−926.

(22) Hogner, A.; Greenwood, J. R.; Liljefors, T.; Lunn, M.; Egebjerg, J.; Larsen, I. K., Gouaux, E.; Kastrup, J. S. Competitive antagonism of AMPA receptors by ligands of different classes: crystal structure of ATPO bound to the GluR2 ligand-binding core, in comparison with DNQX. *J. Med. Chem.* **2003**, *46*, 214−21.

(23) Jin, R.; Banke, T. G.; Mayer, M. L.; Traynelis, S. F.; Gouaux, E. Structural basis for partial agonist action at ionotropic glutamate receptors. *Nat. Neurosci.* **2003**, *6*, 803−810.

(24) Schoepp, D. D.; Lodge, D.; Bleakman, D.; Leander, J. D.; Tizzano, J. P.; Wright, R. A.; Palmer, A. J.; Salhoff, C. R.; Ornstein, P. L. *In vitro* and *in vivo* antagonism of AMPA receptor activation by (3S,4aR,6R,8aR)-6-[2-(1-2H-tetrazole-5-yl)ethyl]decahydroisoquinoiline-3-carboxylic acid. *Neuropharmacology* **1995**, *34*, 1159−1168.

(25) Bleakman, D.; Schoepp, D. D.; Ballyk, B.; Sharpe, E. F.; Bufton, H. R.; Thomas, K.; Ornstein, P. L.; Kamboj, R. K. Pharmacological discrimination of GluR5 and GluR6 kainate receptor subtypes by (3S,4aR,6R,8aR)-6-[2-(1(2)H-tetrazole-5-yl)ethyl]decahydroisoquinoline-3-carboxylic acid. *Mol. Pharmacol.* **1996**, *49*, 581−585.

(26) (a) Jones, K. A.; Wilding, T. J.; Huettner, J. E.; Costa, A. M. Desensitization of kainate receptors by kainate, glutamate and diastereomers of 4-methylglutamate. *Neuropharmacology* **1997**, *36*, 853−863. (b) Zhou, L. M.; Gu, Z. Q.; Costa, A. M.; Yamada, K. A.; Mansson, P. E.; Giordano, T.; Skolnick, P.; Jones, K. A. (2S,4R)-4-methylglutamic acid (SYM 2081): a selective, high-affinity ligand for kainate receptors. *J. Pharmacol. Exp. Ther.* **1997**, *280*, 422−427.

(27) Jones, S. C.; Troop, H. M.; Jane, D. E.; Roberts, P. J. Pharmacological characterization of novel AMPA receptor ligands in rat brain. *Br. J. Pharmacol.* **2001**, *134*, 145P.

(28) Brehm, L.; Greenwood, J. R.; Hansen, K. B.; Nielsen, B.; Egebjerg, J.; Stensbøl, T. B.; ‡Bräuner-Osborne, H.; Sløk, F. A.; Kronborg, T. T. A.; Povl Krogsgaard-Larsen, P. (*S*)-2-Amino-3-(3-hydroxy-7,8-dihydro-6*H*-cyclohepta[*d*]isoxazol-4-yl)propionic Acid, a potent and selective agonist at the GluR5 subtype of ionotropic glutamate receptors. Synthesis, modeling, and molecular pharmacology. *J. Med. Chem.* **2003**, *46*, 1350−1358.

(29) Swanson, G. T.; Green, T.; Heinemann, S. F. Kainate receptors exhibit differential sensitivities to (*S*)-5-iodowillardiine. *Mol. Pharmacol.* **1998**, *53*, 942−949.

(30) Brown, D. J.; Hoerger, E.; Mason, S. F. Simple pyrimidines. Part II. 1:2-Dihydro-1-methylpyrimidines and the configuration of the N-methyluracils. *J. Chem. Soc.* **1955**, *1*, 211−217.

(31) Singh, H.; Aggarwal, P.; Kumar, S. A facile synthesis of 1-monosubstituted and unsymmetrically 1,3-disubstituted uracils. *Synthesis* **1990**, 520−522.

(32) Barrett, H. W.; Goodman, I.; Dittmer, K. Synthesis of 5-halogeno-2-thiouracil and 6-methyl-5-halogeno-2-thiouracil derivatives. *J. Am. Chem. Soc*. **1948**, *70*, 1753−1756.

(33) Ueda, T.; Fox, J. J. Pyrimidines. III. A novel rearrangement in the synthesis of imidazo-or pyrimido[1,2-c]pyrimidines. *J. Org. Chem*. **1964**, *29*, 1762−1769.

(34) Novacek, A.; Lissnerova, M. Nucleic acid components and their analogues. CVII. Cyanoethylation of the uracil and 2-thiouracil derivatives. *Collect. Czech. Chem. Commun*. **1968**, *33*, 604−609.

(35) Atkinson, M. R.; Maguire, M. H.; Ralph, R. K.; Shaw, G.; Warrener, R. N. Purines, pyrimidines and glyoxalines. Part V. New syntheses of uracils and orotic acids. *J. Chem. Soc*. **1957**, *2*, 2363−2368.

(36) Evans, R. H.; Francis, A. A.; Jones, A. W.; Smith, D. A. S.; Watkins, J. C. The effects of a series of ω-phosphonic α-carboxylic amino acids on electrically evoked and excitant amino acid-induced responses in isolated spinal cord preparations. *Br. J. Pharmacol.* **1982**, *75*, 65−75.

(37) Korczak, B.; Nutt, S. L.; Fletcher, E. J.; Hoo, K. H.; Elliott, C. E.; Rampersad, V.; McWhinnie, E. A.; Kamboj, R. K. cDNA cloning and functional properties of human glutamate receptor EAA3 (GluR5) in homomeric and heteromeric configuration. *Recept. Channels* **1995**, *3*, 41−49.

(38) Hoo, K. H.; Nutt, S. L.; Fletcher, E. J.; Elliott, C. E.; Korczak, B.; Deverill, R. M.; Rampersad, V.; Fantaske, R. P.; Kamboj, R. K. Functional expression and pharmacological characterization of the human EAA4 (GluR6) glutamate receptor: a kainate selective channel subunit. *Recept. Channels* **1994**, *2*, 327−337.

(39) Bleakman, D.; Ogden, A. M.; Ornstein, P. L.; Hoo, K. Pharmacological characterization of a GluR6 kainate receptor in cultured hippocampal neurons. *Eur. J. Pharmacol.* **1999**, *378*, 331−337.

(40) Paternain, A. V.; Rodriguez-Moreno, A.; Villarroel, A.; Lerma, J. Activation and desensitization properties of native and recombinant kainate receptors. *Neuropharmacology* **1998**, *37*, 1249−1259.
(41) Cheng, Y. C.; Prusoff, W. H. Relationship between the inhibition constant (K_i) and the concentration of inhibitor which causes 50 per cent inhibition (I_{50}) of an enzymatic reaction. *Biochem. Pharmacol.* **1973**, *22*, 3099−3108.
(42) Alt, A.; Weiss, B.; Ogden, A. M.; Knauss, J. L.; Oler, J.; Ho, K.; Large, T. H.; Bleakman, D. Pharmacological characterization of glutamatergic agonists and antagonists at recombinant human homomeric and heteromeric kainate receptors in vitro. *Neuropharmacology* **2005**, *46*, 793−806.
(43) Pook, P.; Brugger, F.; Hawkins, N. S.; Clark, K. C.; Watkins, J. C.; Evans, R. H. A comparison of the actions of agonists and antagonists at non-NMDA receptors of C fibres and motoneurones of the immature rat spinal cord *in vitro*. *Br. J. Pharmacol.* **1993**, *108*, 179−184.

JM050584L